


Nonequilibrium dynamics of the anyonic Tonks-Girardeau gas at finite temperatureOvidiu I. Pătu *Institute for Space Sciences, Bucharest-Măgurele, R 077125, Romania*

(Received 18 June 2020; accepted 15 September 2020; published 2 October 2020)

We derive an exact description of the nonequilibrium dynamics at finite temperature for the anyonic Tonks-Girardeau gas, extending the results of Atas *et al.* [*Phys. Rev. A* **95**, 043622 (2017)] to the case of arbitrary statistics. The one-particle reduced density matrix is expressed as the Fredholm minor of an integral operator, with the kernel being the one-particle Green's function of free fermions at finite temperature and the statistics parameter determining the constant in front of the integral operator. We show that the numerical evaluation of this representation using Nyström's method significantly outperforms the other approaches present in the literature when there are no analytical expressions for the overlaps of the wave functions. We illustrate the distinctive features and novel phenomena present in the dynamics of anyonic systems in two experimentally relevant scenarios: the quantum Newton's cradle setting and the breathing oscillations initiated by a sudden change of the trap frequency.

DOI: [10.1103/PhysRevA.102.043303](https://doi.org/10.1103/PhysRevA.102.043303)**I. INTRODUCTION**

In recent years considerable efforts have been made in order to understand the principles underlying the nonequilibrium dynamics of integrable and nonintegrable isolated many-body systems. The results of a large body of literature can be succinctly summarized as follows. After a quench, nonintegrable (chaotic) systems are described in the long-time limit by a Gibbs (thermal) ensemble [1–3]. Integrable systems, however, fail to thermalize, and their asymptotic properties are described by a generalized Gibbs ensemble (GGE) [4,5] which needs to take into account all the local and quasilocal integrals of motion of the system [6–8]. In the case of near-integrable systems we encounter the phenomenon of prethermalization [9–16], which is characterized by a quasistationary state with almost integrable features at short to moderate times, reaching thermal equilibrium only after very long time.

The main impetus behind these theoretical developments was a series of experiments with ultracold atomic gases [17–25], of which the quantum Newton's cradle (QNC) experiment of Kinoshita *et al.* [26] stands out. Trapped ultracold atomic gases represent the perfect testing ground for the investigation of nonequilibrium dynamics of quantum many-body systems due to their unprecedented level of control of control over interactions, dimensionality, and even statistics, which allows for the realization of integrable and nonintegrable systems which can be accurately monitored over long timescales. In addition, these systems are also characterized by weak coupling to their environment, which means that to a good approximation they can be considered as isolated.

One of the most important models that can be realized with ultracold atoms is the Lieb-Liniger model [27], which describes one-dimensional bosons with repulsive contact in-

teractions. In a homogeneous system and for arbitrary values of the repulsion, the Lieb-Liniger model is integrable and the wave functions, energy spectrum, and low-lying excitations can be obtained using the Bethe ansatz [27–29]. In typical experiments the system is confined to one dimension by using a strong transverse optical trap, while in the longitudinal direction there is a harmonic potential which breaks integrability. In the limit of infinite repulsion between the particles, the Lieb-Liniger model describes the so-called Tonks-Girardeau gas [30], which is integrable in both homogeneous and inhomogeneous cases using Bose-Fermi mapping [30–36].

A natural generalization of the Lieb-Liniger model in the case of arbitrary statistics is given by the anyonic Lieb-Liniger model introduced in [37] (see also [38,39]). This model has been studied intensely in the last decade, and a large body of knowledge has been steadily accumulating, including the properties of the ground state [38,40], form factors [41], the asymptotic behavior of the correlation functions for homogeneous [42–47] and trapped systems [48–50], and entanglement [51,52]. The nonequilibrium properties after particular quenches at zero temperature were studied in [53–55]. Experimental proposals of realizing one-dimensional (1D) anyonic systems with ultracold atoms in optical lattices using various methods such as Raman-assisted tunneling [56,57], periodically driven lattices [58], or multicolor lattice-depth modulation [59,60] have reignited interest in the study of systems with fractional statistics [61–95].

The majority of the analytical and numerical investigations of the nonequilibrium dynamics in the literature treat the case of zero temperature. However, experiments are realized at nonzero temperatures, and therefore it is important to have analytical tools to study finite temperature dynamics. Another reason why it is important to derive finite-temperature results is to establish *a priori* bounds on the physical parameters

for which phenomena predicted at zero or low temperatures can still be seen and not be washed out by thermal fluctuations.

In this paper we investigate the finite-temperature dynamics of the anyonic Tonks-Girardeau gas focusing on two experimentally relevant scenarios: the quantum Newton’s cradle setting and the breathing-mode oscillations after a quench of the trap frequency. At first glance it would seem that the knowledge of the wave functions, which can be obtained using the Anyon-Fermi mapping [64,65], would make the task of computing physical relevant observables like the momentum distribution an easy one. This is, however, an unwarranted assumption due to the fact that a brute force approach of computing the one-particle reduced density matrix (RDM) requires a computational cost which increases exponentially with the number of particles. A numerical efficient method to compute the dynamical RDM of impenetrable bosons at zero temperature was derived by Pezer and Buljan in [96]. The main computational cost of this method is represented by the calculation of the determinant and inverse of a matrix whose dimension is equal to the number of particles, and the elements are given by the overlaps of the wave functions. This method is extremely efficient when the overlaps can be computed analytically, and it was extended in the anyonic case by del Campo in [53].

The generalization for impenetrable bosons at finite temperature was introduced rather recently by Atas *et al.* in [97] (for the so-called “emergent eigenstate solution” of the bosonic Tonks-Girardeau (TG) gas valid at any temperature see [98]). They considered that in the initial state the system is described by a grand-canonical ensemble and made use of Lenard’s formula [99], which expresses the RDMs of bosons in terms of an infinite series involving the RDMs of free fermions. This series in the case of the one-particle RDM is the first Fredholm minor of an integral operator with the kernel given by the one-particle RDM of free fermions at finite temperature. Truncating the expression for the free fermionic RDM after a finite number of terms (this is perfectly justified because each term is multiplied by the Fermi-Dirac occupation factor), the authors of [97] were able to obtain an expression for the bosonic RDM which is almost identical with that derived at zero temperature in [96] with two differences: the wave function overlaps are now “dressed” with the square root of the Fermi-Dirac occupation factors, and the dimension of the matrix now is equal with the truncation level. Our derivation presented in this paper in the case of the anyonic Tonks-Girardeau gas follows along similar lines and makes use of the anyonic generalization of Lenard’s formula [65], but for the numerical treatment we prefer a different approach. When the overlaps can be calculated analytically, the numerical method derived in [97] is almost always preferable; however, when this is not possible, which is the case in many physical relevant situations like in the QNC setting, a more efficient numerical method is based on the evaluation of the Fredholm minor using Nyström’s method [100,101]. A detailed comparison of the two methods can be found in Appendix D, where it is shown that for moderate or large number of particles and especially at finite temperatures, Nyström’s method can be even several orders of magnitude faster than the overlap approach.

Similar to the bosonic analysis in [97], we consider the nonequilibrium dynamics in two interesting and experimentally relevant situations. In the QNC setup the application of the Bragg pulse (we use the Bragg pulse modeling introduced in [31,102]) produces a nonsymmetric momentum distribution which is a distinct feature of anyonic systems [40,44,53,85]. In [102], which treated the bosonic case, two different timescales were discovered: one of rapid trap-insensitive relaxation right after the application of the pulse followed by slow periodic behavior. This separation of timescales is also present in the anyonic system. During the periodic behavior the momentum distribution presents alternatively fermionic and anyonic characteristics. This phenomenon, which we call “periodic dynamical fermionization,” is even more pronounced in the dynamics of the anyonic gas after a quantum quench of the trapping frequency, which produces breathing-mode oscillations. In this case we also observe another many-body collective effect similar to the one discovered in [103] for the bosonic Tonks-Girardeau gas, which is characterized by an additional narrowing of the momentum distribution when the gas is maximally compressed. In the anyonic case this narrowing decreases as the statistics parameter increases ($\kappa = 0$ for bosons and $\kappa = 1$ for fermions) and eventually disappears for the fermionic system.

The plan of the paper is as follows. In Secs. II and III we introduce the anyonic Tonks-Girardeau model, its eigenfunctions, and the one-particle RDM. The derivation of the anyonic generalization of Lenard’s formula is presented in Sec. IV, and the details of the two numerical methods can be found in Sec. V. The nonequilibrium dynamics in the QNC setup and after a quantum quench of the trap frequency is studied in Secs. VI and VII. We conclude in Sec. VIII. Some information about the Fredholm minors, the RDMs of free fermions, and two useful theorems are presented in Appendixes A, B, and C. A detailed comparison of the two numerical methods used in this paper can be found in Appendix D.

II. THE ANYONIC TONKS-GIRARDEAU GAS

We consider a one-dimensional system of N anyons interacting via a repulsive δ -function potential in the presence of a confining time-dependent external potential. The second quantized Hamiltonian is

$$\mathcal{H} = \int dx \frac{\hbar^2}{2m} (\partial_x \Psi^\dagger)(\partial_x \Psi) + g \Psi^\dagger \Psi^\dagger \Psi \Psi + V(x, t) \Psi^\dagger \Psi, \quad (1)$$

with the anyonic fields $\Psi^\dagger(x)$, $\Psi(x)$ satisfying the following commutation relations:

$$\Psi(x) \Psi^\dagger(y) = e^{-i\pi\kappa\varepsilon(x-y)} \Psi^\dagger(y) \Psi(x) + \delta(x-y), \quad (2a)$$

$$\Psi(x) \Psi(y) = e^{i\pi\kappa\varepsilon(x-y)} \Psi(y) \Psi(x), \quad (2b)$$

with $\kappa \in [0, 1]$ the statistics parameter and $\varepsilon(x) = |x|/x$, $\varepsilon(0) = 0$. Varying the statistics parameter κ in the $[0,1]$ interval and for $x \neq y$ the anyonic commutation relations (2) interpolate continuously between the canonical commutation relations for bosons ($\kappa = 0$) and the canonical anticommutation relations for fermions ($\kappa = 1$). At coinciding points, $x = y$, the commutation relations are

bosonic in nature. We should point out that an equally valid choice of interval for the variation of the statistics parameter is given by $\kappa \in [-1, 0]$ with the fermionic system described by $\kappa = -1$. In (1) \hbar is the reduced Planck constant, m is the mass of the particles, g quantifies the strength of the repulsive interaction, and $V(x, t)$ is the time-dependent external potential. We are going to mainly consider the case of the parabolic confining potential with time-dependent frequency $V(x, t) = m\omega^2(t)x^2/2$, but the considerations of this section are also valid in the case of more complicated time-dependent external potentials.

When $V(x, t) = 0$ the Hamiltonian (1) describes the integrable anyonic Lieb-Liniger model [37,38,43], which is the natural generalization to arbitrary statistics of the bosonic Lieb-Liniger model [27]. Introducing the Fock vacuum $|0\rangle$ defined by $\Psi(x)|0\rangle = \langle 0|\Psi^\dagger(x) = 0$ for all x and $\langle 0|0\rangle = 1$ the eigenstates of the Hamiltonian (1) are

$$|\psi_N(t)\rangle = \frac{1}{\sqrt{N!}} \int dz_1 \cdots dz_N \psi_{N,A}(z_1, \dots, z_N|t) \times \Psi^\dagger(z_N, t) \cdots \Psi^\dagger(z_1, t)|0\rangle, \quad (3)$$

with $\Psi^\dagger(z, t) = e^{i\hbar t} \Psi^\dagger(z) e^{-i\hbar t}$. The N -body anyonic wave function $\psi_{N,A}$ satisfies

$$\psi_{N,A}(\dots, z_i, z_{i+1}, \dots |t) = e^{i\pi\kappa\varepsilon(z_i - z_{i+1})} \times \psi_{N,A}(\dots, z_{i+1}, z_i, \dots |t). \quad (4)$$

This shows that the wave function is symmetric under the permutation of two particles when the system is bosonic ($\kappa = 0$) and antisymmetric when the system is fermionic ($\kappa = 1$). For an anyonic system, $\kappa \in (0, 1)$, the previous relation reveals the broken space-reversal symmetry characteristic of 1D anyons, which results in a nonsymmetric momentum distribution.

The first quantized version of (1) is

$$H = \sum_{i=1}^N \left[-\frac{\hbar^2}{2m} \frac{\partial^2}{\partial z_i^2} + V(z_i, t) \right] + 2g \sum_{1 \leq i < j \leq N} \delta(z_i - z_j), \quad (5)$$

and in this paper we are going to consider the Tonks-Girardeau limit ($g \rightarrow \infty$) of the Hamiltonian (5), which imposes an additional hard-core constraint on the wave function of the anyonic system $\psi_{N,A}(\dots, z, \dots, z, \dots) = 0$. In this limit the anyonic system described by (5) can be investigated by considering a dual system of N free fermions described by the Hamiltonian

$$H_F = \sum_{i=1}^N \left[-\frac{\hbar^2}{2m} \frac{\partial^2}{\partial z_i^2} + V(z_i, t) \right], \quad (6)$$

and the wave functions can be determined employing the Anyon-Fermi mapping [64,65] [$\mathbf{z} = (z_1, \dots, z_N)$]:

$$\psi_{N,A,\nu}(\mathbf{z}|t) = A(\mathbf{z})B(\mathbf{z})\psi_{N,F,\nu}(\mathbf{z}|t), \quad (7)$$

where

$$A(\mathbf{z}) = \prod_{j < k} e^{i\frac{\pi\kappa}{2}\varepsilon(z_j - z_k)}, \quad B(\mathbf{z}) = \prod_{j > k} \varepsilon(z_j - z_k), \quad (8)$$

and $\psi_{N,F,\nu}(\mathbf{z}|t)$ are the wave functions of the dual fermionic system. In (7) the wave functions also depend on $\nu = (\nu_1, \dots, \nu_N)$, which identify the single-particle energy levels. The fermionic wave functions are Slater determinants [which are eigenstates of (6) and constitute a basis of the Fock space] of the single-particle (SP) wave functions

$$\psi_{N,F,\nu}(\mathbf{z}|t) = \frac{1}{\sqrt{N!}} \det_{i,j=1}^N \phi_{\nu_i}(z_j, t), \quad (9)$$

where $H_{SP}(z, 0)\phi_{\nu_i}(z) = E_{\nu_i}\phi_{\nu_i}(z)$ and $i\hbar\partial\phi_{\nu_i}(z, t)/\partial t = H_{SP}(z, t)\phi_{\nu_i}(z, t)$ with $H_{SP}(z, t) = -(\hbar^2/2m)(\partial^2/\partial z^2) + V(z, t)$. At $t = 0$ the energy of the N -body state (9) is $E_{N,\nu} = \sum_{i=1}^N E_{\nu_i}$.

We should point out that the Anyon-Fermi mapping remains valid even in the case of a general potential energy as long as it includes a hard core of radius $a \geq 0$ [65,99]. In the case of hard-wall boundary conditions or when the systems are subjected to a confining external potential, the same boundary conditions hold for the anyonic and fermionic systems and the energy eigenvalues are equal. In the case of periodic or twisted boundary conditions the situation is more complicated (see [65,99]).

III. ONE-BODY REDUCED DENSITY MATRIX

In this paper we are interested in investigating the dynamics of the anyonic one-body reduced density matrix at finite temperature defined by $[\bar{\mathbf{z}} = (z_1, \dots, z_{N-1})]$

$$\rho^{(1)}(x, y|t) = \sum_{N=1}^{\infty} \sum_{\nu} p(N, \nu) N \int dz_1 \cdots dz_{N-1} \times \psi_{N,A,\nu}(\bar{\mathbf{z}}, x|t) \psi_{N,A,\nu}^*(\bar{\mathbf{z}}, y|t), \quad (10)$$

with $p(N, \nu)$ the probabilities of an arbitrary statistical ensemble. Following [97] (see also [104] for the lattice case), we consider the system initially in thermal equilibrium described by the grand-canonical ensemble with $p(N, \nu) = e^{-(E_{N,\nu} - \mu N)/k_B T_0} / \mathcal{Z}$, μ the chemical potential, and T_0 the equilibrium temperature at $t = 0$. $\mathcal{Z} = \sum_{N,\nu} e^{-(E_{N,\nu} - \mu N)/k_B T_0}$ is the grand-canonical partition function, and $\psi_{N,A,\nu}(\bar{\mathbf{z}}, x|t)$ are the evolved wave functions obtained from $\psi_{N,A,\nu}(\bar{\mathbf{z}}, x|0)$ with the Hamiltonian (5). From the one-body density matrix we can obtain two very important and experimentally accessible quantities: the real-space density $\rho(x, t) = \rho^{(1)}(x, x|t)$ and the momentum distribution

$$n(k, t) = \iint e^{-ik(x-y)} \rho^{(1)}(x, y|t) dx dy. \quad (11)$$

We should point out that while the real-space density is independent of the statistics [this can be seen easily from the Anyon-Fermi mapping (7) and (10)], the momentum distribution is highly dependent on κ .

IV. ANYONIC GENERALIZATION OF LENARD'S FORMULA

In the 1960s Lenard used the Bose-Fermi mapping to derive an expansion of the bosonic reduced density matrices in terms of the fermionic reduced matrices [99]. Lenard's result is valid not only for the one-body RDM but also for the more general case of the n -body density matrices defined by

$$\rho^{(n)}(\mathbf{x}, \mathbf{y} | t) = \sum_{N=n}^{\infty} \sum_{\mathbf{v}} p(N, \mathbf{v}) \frac{N!}{(N-n)!} \int dz_1 \cdots dz_{N-n} \psi_{N,A,\mathbf{v}}(z, \mathbf{x} | t) \psi_{N,A,\mathbf{v}}^*(z, \mathbf{y} | t), \tag{12}$$

with $\mathbf{x} = (x_1, \dots, x_n)$, $\mathbf{y} = (y_1, \dots, y_n)$, and $\bar{z} = (z_1, \dots, z_{N-n})$. The anyonic generalization of Lenard's formula was derived in [65]. In order to make the paper self-contained, here we rederive it in the particular case of the one-body density matrix. We will need a simple result [65,99].

Lemma 1. For any symmetric function $f(z_1, \dots, z_n)$, a constant ξ , and I an interval in the domain Ω we have

$$\int_{\Omega} dz_1 \cdots \int_{\Omega} dz_n \xi^{\sigma(I)} f(z_1, \dots, z_n) = \sum_{j=0}^n C_j^n (-1 + \xi)^j \int_I dz_1 \cdots \int_I dz_j \int_{\Omega} dz_{j+1} \cdots \int_{\Omega} dz_n f(z_1, \dots, z_n), \tag{13}$$

where $\sigma(I)$ counts the number of variables z_1, \dots, z_n contained in I .

We start from the definition of the reduced density matrix (10). Using the Anyon-Fermi mapping (7) for the wave functions we have

$$\begin{aligned} \psi_{N,A,\mathbf{v}}(\bar{z}, \mathbf{x} | t) \psi_{N,A,\mathbf{v}}^*(\bar{z}, \mathbf{y} | t) &= \prod_{1 \leq j \leq N-1} [e^{i\frac{\pi\xi}{2} [\varepsilon(z_j-x) - \varepsilon(z_j-y)]} \varepsilon(x - z_j) \varepsilon(y - z_j)] \psi_{N,F,\mathbf{v}}(\bar{z}, \mathbf{x} | t) \psi_{N,F,\mathbf{v}}^*(\bar{z}, \mathbf{y} | t), \\ &= (-e^{i\pi\kappa\varepsilon(y-x)})^{\sigma(I)} \psi_{N,F,\mathbf{v}}(\bar{z}, \mathbf{x} | t) \psi_{N,F,\mathbf{v}}^*(\bar{z}, \mathbf{y} | t), \end{aligned} \tag{14}$$

with $\bar{z} = (z_1, \dots, z_{N-1})$ and $I = [x, y]$ when $y > x$ and $I = [y, x]$ when $x > y$. Introducing $\xi = -e^{i\pi\kappa\varepsilon(y-x)}$ and plugging the previous result in (10) followed by the application of the Lemma 1 we find

$$\begin{aligned} \rho^{(1)}(x, y | t) &= \sum_{N=1}^{\infty} \sum_{\mathbf{v}} p(N, \mathbf{v}) N \int dz_1 \cdots dz_{N-1} \xi^{\sigma(I)} \psi_{N,F,\mathbf{v}}(\bar{z}, \mathbf{x} | t) \psi_{N,F,\mathbf{v}}^*(\bar{z}, \mathbf{y} | t), \\ &= \sum_{N=1}^{\infty} \sum_{\mathbf{v}} p(N, \mathbf{v}) N \left(\sum_{j=0}^{N-1} C_j^{N-1} (-1 + \xi)^j \int_I dz_1 \cdots \int_I dz_j \int dz_{j+1} \cdots \int dz_{N-1} \psi_{N,F,\mathbf{v}}(\bar{z}, \mathbf{x} | t) \psi_{N,F,\mathbf{v}}^*(\bar{z}, \mathbf{y} | t) \right). \end{aligned}$$

In the last relation changing the order of the summation we can identify in the right-hand side the reduced density matrices of free fermions, denoted by $\rho_F^{(n)}$ [for an alternative definition equivalent with (12) in the case of fermions see (B1)], obtaining

$$\begin{aligned} \rho^{(1)}(x, y | t) &= \sum_{j=0}^{\infty} \frac{(-1 + \xi)^j}{j!} \int_I dz_1 \cdots \int_I dz_j \rho_F^{(j+1)}(z_1, \dots, z_j, x; z_1, \dots, z_j, y | t), \\ &= \sum_{j=0}^{\infty} \frac{(-1 + \xi)^j}{j!} [\varepsilon(y-x)]^j \int_x^y dz_1 \cdots \int_x^y dz_j \rho_F^{(j+1)}(z_1, \dots, z_j, x; z_1, \dots, z_j, y | t). \end{aligned} \tag{15}$$

The reduced density matrices of free fermions are computed in Appendix B. Using formula (B10) in (15) we obtain the main result of this section: the anyonic generalization of Lenard's formula for the one-body RDM is

$$\rho^{(1)}(x, y | t) = \sum_{j=0}^{\infty} \frac{(-\gamma)^j}{j!} \int_x^y dz_1 \cdots \int_x^y dz_j \rho_F^{(1)} \left(\begin{matrix} x & z_1 & \cdots & z_j \\ y & z_1 & \cdots & z_j \end{matrix}; t \right), \quad \gamma = \varepsilon(y-x)(1 + e^{i\pi\kappa\varepsilon(y-x)}), \tag{16}$$

where we have used the notation introduced in (A3) and $\rho_F^{(1)}(x, y | t) = \sum_{i=0}^{\infty} f_i \phi_i(x, t) \phi_i^*(y, t)$ with $f_i = [e^{(E_i - \mu)/k_B T_0} + 1]^{-1}$ the Fermi-Dirac occupation factor. The $j = 0$ term of (16) is given by $\rho_F^{(1)}(x, y | t)$, which is the one-body reduced density matrix of the dual fermionic system.

V. FREDHOLM MINOR REPRESENTATION FOR THE REDUCED DENSITY MATRIX

While it is useful to derive the short distance expansion of the one-body RDM [105–107], the numerical implementation of Lenard's formula (16) is computationally involved, even if we truncate the series after the first few terms. The efficient calculation of physical relevant quantities, such as

the momentum distribution, and not only for large values of k , requires a more computationally friendly representation of (16). A more fruitful approach is to realize that (16) is the first Fredholm minor [see formula (A5)] of an integral operator $1 - \gamma \hat{\rho}_F^{(1)}$ with kernel $\rho_F^{(1)}(\lambda, \mu | t)$, which acts on an arbitrary function like $\int_x^y \rho_F^{(1)}(\lambda, \mu | t) f(\mu) d\mu$ and γ is defined in (16) [99,106,107]. Introducing the resolvent kernel

of this integral operator, which satisfies

$$\mathbf{R}_F(\lambda, \mu|t) = \rho_F^{(1)}(\lambda, \mu|t) + \gamma \int_x^y \rho_F^{(1)}(\lambda, \nu|t) \mathbf{R}_F(\nu, \mu|t) d\nu, \quad (17)$$

and using the identity (A8) we find

$$\rho_F^{(1)}(x, y|t) = \mathbf{R}_F(x, y|t) \det(1 - \gamma \hat{\rho}_F^{(1)}). \quad (18)$$

The representation (18) for arbitrary statistics was first derived in [65]. An efficient numerical evaluation of (18) [or, equivalently, of (16)] in the case of impenetrable bosons at zero temperature was proposed by Pezer and Buljan in [96] and in the case of arbitrary statistics by del Campo in [53]. The finite-temperature generalization for impenetrable bosons was derived by Atas *et al.* in [97]. In this paper we are going to use another approach based on the numerical evaluation of the resolvent and Fredholm determinant using Nyström's method [100,101]. In addition, we will also derive the anyonic generalization of the result obtained in [97]. In Appendix D we show that when there is no analytical formula for the overlaps of the single-particle wave functions (which is the case in many experimentally relevant cases such as the QNC setup), this approach significantly outperforms the methods of [96] and [97] for moderate and large number of particles at zero and finite temperatures.

The starting point of both methods is represented by the truncation of the sum which describes the free fermionic one-body density matrix after the first M terms:

$$\rho_F^{(1)}(x, y|t) \simeq \sum_{i=0}^{M-1} f_i \phi_i(x, t) \phi_i^*(y, t). \quad (19)$$

The truncation parameter M has to be chosen such that the discarded terms in the infinite sum are negligible. At zero temperature we have $M = N$, with N the number of particles in the system and $\rho_F^{(1)}(x, y|t) = \sum_{i=0}^{N-1} \phi_i(x, t) \phi_i^*(y, t)$. It is also assumed that the SP wave functions $\{\phi_i(x, t)\}_{i=0}^{M-1}$ are known either analytically or by numerically solving the time-dependent Schrödinger equation.

A. Numerical evaluation of the RDM using Nyström's method

Assuming that we know the one-body RDM of free fermions $\rho_F^{(1)}(\lambda, \mu|t)$, probably the simplest method of evaluating (18) is by solving the integral equation satisfied by the resolvent (17) followed by the evaluation of the Fredholm determinant. Equation (17) is a Fredholm integral equation of the second kind with a smooth kernel which can be very easily and accurately solved using Nyström's method (Chap. 18 of [100]), and, as it was shown in [101], the same method can be used to evaluate the Fredholm determinant. Briefly, the necessary steps are the following. Consider a quadrature (for a pragmatic introduction in numerical integration with quadratures, see Chap. 4 of [100]) with positive weights which approximates the integral over $[x, y]$ of an arbitrary function $f(\lambda)$ (reasonably well behaved) as

$$\int_x^y f(\lambda) d\lambda \simeq \sum_{j=1}^m w_j f(\lambda_j). \quad (20)$$

In (20) $\{w_j\}_{j=1}^m$ are called the quadrature weights and $\{\lambda_j\}_{j=1}^m$ the quadrature points or abscissas. Using this quadrature the integral equation (17) for $\mu = y$ can be written as

$$\mathbf{R}_F(\lambda, y|t) = \rho_F^{(1)}(\lambda, y|t) + \gamma \sum_{j=1}^m w_j \rho_F^{(1)}(\lambda, \lambda_j|t) \mathbf{R}_F(\lambda_j, y|t). \quad (21)$$

Considering (21) at all points of the quadrature $\{\lambda_j\}_{j=1}^m$ we obtain the following system of m linear equations:

$$(1 - \gamma \bar{\rho}_F^{(1)}) R = \rho, \quad (22)$$

with $\bar{\rho}_F^{(1)}$ a square matrix of dimension m and elements $w_j \rho_F^{(1)}(\lambda_i, \lambda_j|t)$ and

$$R = [\mathbf{R}_F(\lambda_1, y|t), \dots, \mathbf{R}_F(\lambda_m, y|t)]^T, \quad \rho = [\rho_F^{(1)}(\lambda_1, y|t), \dots, \rho_F^{(1)}(\lambda_m, y|t)]^T. \quad (23)$$

Then $R = (1 - \gamma \bar{\rho}_F^{(1)})^{-1} \rho$ and $\mathbf{R}_F(x, y|t)$ can be computed using the solution for R and (21) for $\lambda = x$. Therefore, for the computation of $\mathbf{R}_F(x, y|t)$ we need only to solve the system of linear equations (22), followed by the use of the interpolation formula (21). The evaluation of the Fredholm determinant is even simpler [101] and is given by

$$\det(1 - \gamma \hat{\rho}_F^{(1)}) = \det(\delta_{ij} - \gamma w_i^{1/2} \rho_F^{(1)}(\lambda_i, \lambda_j|t) w_j^{1/2})_{i,j=1}^m. \quad (24)$$

We make two observations. First, the outlined derivation does not depend explicitly on the truncation level M , so in principle it is also valid if we would know the free fermionic RDM through other methods and not from (19). Second, it is also valid at zero temperature. In this case Eq. (19) reduces to its zero-temperature expression.

In summary, the numerical evaluation of the reduced density matrix (18) using Nyström's method consists of the following steps: (a) determination (analytically or numerically) of the SP wave functions $\{\phi_i(x, t)\}_{i=0}^{M-1}$; (b) solving the linear system (22) with the free fermionic RDM given by (19); (c) determination of $\mathbf{R}_F(x, y|t)$ using the solution of the linear system and interpolation formula (21); and (d) computation of the Fredholm determinant using (24).

B. Numerical evaluation of the RDM using the truncated basis

In this section we are going to obtain the generalization to arbitrary statistics of the numerical method derived in [97] for impenetrable bosons. It will be useful to introduce the notation

$$\tilde{\phi}_i(\lambda, t) = \sqrt{f_{i-1}} \phi_{i-1}(\lambda, t), \quad i = 1, \dots, M, \quad (25)$$

in terms of which (19) takes the form $\rho_F^{(1)}(\lambda, \mu|t) = \sum_{i=1}^M \tilde{\phi}_i(\lambda, t) \tilde{\phi}_i^*(\mu, t)$. We want to obtain numerically manageable expressions for the resolvent and Fredholm determinant in the truncated basis $\{\tilde{\phi}_i(\lambda, t)\}_{i=1}^M$.

Resolvent kernel in the truncated basis. By plugging the truncated expression for $\rho_F^{(1)}(\lambda, \mu|t)$ in the integral equation

satisfied by the resolvent kernel Eq. (17) we obtain

$$R_F(\lambda, \mu|t) = \sum_{j=1}^M \tilde{\phi}_j(\lambda, t) \tilde{\phi}_j^*(\mu, t) + \gamma \sum_{j=1}^M \tilde{\phi}_j(\lambda, t) A_j(\mu, t), \quad (26)$$

where we have introduced

$$A_j(\mu, t) = \int_x^y \tilde{\phi}_j^*(\nu, t) R_F(\nu, \mu|t) d\nu.$$

The A_j coefficients can be determined by multiplying Eq. (26) with $\tilde{\phi}_j^*(\lambda, t)$ and integrating over the $[x, y]$ interval. We find

$$A_j(\mu, t) = \sum_{i=1}^M S_{ij}(t) [\tilde{\phi}_i^*(\mu, t) + \gamma A_i(\mu, t)], \quad (27)$$

with $S(t)$ a square matrix of dimension M with elements

$$S_{ij}(t) = \int_x^y \tilde{\phi}_i(\lambda, t) \tilde{\phi}_j^*(\lambda, t) d\lambda. \quad (28)$$

We want to rewrite the previous results in a matrix form transparent notation. We introduce two column vectors defined by $A = (A_1, \dots, A_M)^T$ and $\tilde{\phi}^* = (\tilde{\phi}_1^*, \dots, \tilde{\phi}_M^*)^T$. Then, (27) can be written as $(1 - \gamma S^T)A = S^T \phi^*$ or, equivalently, as $A = (1 - \gamma S^T)^{-1} S^T \phi^*$. From this last relation and Eq. (26) we see that

$$\begin{aligned} R_F(\lambda, \mu|t) &= \sum_{i,j=1}^M \tilde{\phi}_i(\lambda, t) \\ &\times (\delta_{ij} + \gamma [(1 - \gamma S^T)^{-1} S^T]_{ij}) \tilde{\phi}_j^*(\mu, t), \\ &= \sum_{i,j=1}^M \tilde{\phi}_i(\lambda, t) (1 - \gamma S^T)^{-1}_{ij} \tilde{\phi}_j^*(\mu, t), \end{aligned} \quad (29)$$

which represents the resolvent kernel in the truncated basis.

Fredholm determinant in the truncated basis. Now we are going to show that in the truncated basis we have

$$\det(1 - \gamma \rho_F^{(1)}) = \det(1 - \gamma S). \quad (30)$$

We point out that in the left-hand side of the previous relation we have a Fredholm determinant [see Eq. (A4)], while on the right-hand side we have a usual determinant of a square matrix of dimension M . From the definition of the Fredholm determinant we have [see (A3) and (A4)]

$$\begin{aligned} \det(1 - \gamma \rho_F^{(1)}) &= 1 + \sum_{n=1}^{\infty} \frac{(-\gamma)^n}{n!} \int_x^y d\xi_1 \cdots \int_x^y d\xi_n \\ &\times \rho_F^{(1)}(\xi_1 \cdots \xi_n; t). \end{aligned} \quad (31)$$

On the other hand, using the von Koch formula for the determinant we have

$$\det(1 - \gamma S) = 1 + \sum_{n=1}^M \frac{(-\gamma)^n}{n!} \sum_{k_1, \dots, k_n=1}^M \det(S_{k_p, k_q})_{p,q=1}^n. \quad (32)$$

We will show that (a) all the terms with $n > M$ in the right-hand side of (31) vanish and (b) for all $n \leq M$ the terms in the

expansions (31) and (32) are equal, proving (30). Let $n \leq M$. Then

$$\rho_F^{(1)}(\xi_1 \cdots \xi_n; t) = \begin{vmatrix} a_1^2 & a_1 \cdot a_2 & \cdots & a_1 \cdot a_n \\ a_2 \cdot a_1 & a_2^2 & \cdots & a_2 \cdot a_n \\ \vdots & \vdots & \ddots & \vdots \\ a_n \cdot a_1 & a_n \cdot a_2 & \cdots & a_n^2 \end{vmatrix},$$

with $a_i = [\tilde{\phi}_1(\xi_i, t), \dots, \tilde{\phi}_M(\xi_i, t)]$ and scalar product $a_i \cdot a_j = \sum_{k=1}^M a_{ik} a_{jk}^*$. From this representation we see that the only nonvanishing terms in the expansion are the ones with $n \leq M$. (If $n > M$ we would have on the right-hand side the Gram determinant of a number of vectors which is larger than the dimension of the linear space and therefore is equal to zero.) Using Theorem (1) of Appendix C we obtain

$$\begin{aligned} \rho_F^{(1)}(\xi_1 \cdots \xi_n; t) &= \frac{1}{n!} \sum_{k_1, \dots, k_n=1}^M \begin{vmatrix} a_{1k_1} & a_{1k_2} & \cdots & a_{1k_n} \\ a_{2k_1} & a_{2k_2} & \cdots & a_{2k_n} \\ \vdots & \vdots & \ddots & \vdots \\ a_{nk_1} & a_{nk_2} & \cdots & a_{nk_n} \end{vmatrix}^2, \end{aligned} \quad (33)$$

with $a_{ik} = \tilde{\phi}_k(\xi_i, t)$. In the case of the von Koch expansion (32), employing Theorem 2 of Appendix C we have

$$\begin{aligned} \sum_{k_1, \dots, k_n=1}^M \det(S_{k_p, k_q})_{p,q=1}^n &= \frac{1}{n!} \sum_{k_1, \dots, k_n=1}^M \int_x^y d\xi_1 \cdots \int_x^y d\xi_n \begin{vmatrix} a_{1k_1} & a_{2k_1} & \cdots & a_{nk_1} \\ a_{1k_2} & a_{2k_2} & \cdots & a_{nk_2} \\ \vdots & \vdots & \ddots & \vdots \\ a_{1k_n} & a_{2k_n} & \cdots & a_{nk_n} \end{vmatrix}^2. \end{aligned} \quad (34)$$

Then (30) follows from (34) and (33), and the fact that $\det A = \det A^T$ for an arbitrary square matrix A . An alternative derivation of this result can be obtained using Plemelj's formula for the Fredholm determinant as in [108].

Plugging (29) and (30) in (18) and using $(1 - \gamma S^T)^{-1} = [(1 - \gamma S)^{-1}]^T$ we obtain

$$\rho^{(1)}(x, y|t) = \sum_{i,j=0}^{M-1} \sqrt{f_i} \phi_i(x, t) Q_{ij}(x, y|t) \sqrt{f_j} \phi_j^*(y, t), \quad (35)$$

with

$$Q(x, y|t) = [P^{-1}(x, y|t)]^T \det P(x, y|t). \quad (36)$$

In (35) and (36) Q and P are square matrices of dimension M with indices $i, j = 0, \dots, M - 1$ and the elements of P are

$$P_{ij}(x, y|t) = \delta_{ij} - \gamma \sqrt{f_i f_j} \int_x^y \phi_i(\lambda, t) \phi_j^*(\lambda, t) d\lambda, \quad (37)$$

with $\gamma = \varepsilon(y - x)(1 + e^{i\pi\kappa\varepsilon(y-x)})$.

In the bosonic case ($\kappa = 0$) (35) reproduces the result from [97] and for $\kappa = 1$ it reduces to $\rho^{(1)}(x, y|t) = \sum_{i=0}^{M-1} f_i \phi_i(x, t) \phi_j^*(y, t)$, which is just the free fermionic result as expected. At zero temperature the occupation factors become zero for $M > N - 1$ and we obtain the results derived in [53,96]. The necessary steps required to compute

the RDM of an anyonic system using the method presented in this section are the following: (a) determination of the SP wave functions; (b) calculation of the wave-function overlaps and of the matrix \mathbf{P} using (37); (c) computation of the matrix \mathbf{Q} (36); and (d) performing the summation in (35).

C. Comparison of the two methods

A detailed analysis of the complexity of the two methods outlined above can be found in Appendix D. We have two distinct situations. If the overlaps of the wave functions $\int_x^y \phi_i(\lambda, t) \phi_j^*(\lambda, t) d\lambda$ can be analytically computed then the truncated basis method (35) is the method of choice and will be used in Sec. VII. If the overlaps are not amenable to analytical calculations and numerical integration is required, then Nyström's method is preferable with the exception of the case of a small number of particles (or truncation level M) and large $|x - y|$. In particular, Nyström's method is extremely efficient, especially at finite temperatures (see Appendix D), because (a) M increases with temperature and (b) due to the exponential decay the RDM is concentrated in a narrow strip $|x - y| < C$ with the contributions from $|x - y| > C$ being negligible.

VI. ANYONIC QUANTUM NEWTON'S CRADLE

As a first application of the formalism developed in the previous sections we are studying the dynamics of the anyonic TG gas in the QNC setting at finite temperature. In the original experiment [26] a quasi-1D gas of ^{87}Rb atoms in a weakly harmonical potential in the longitudinal direction was subjected to a sequence of Bragg pulses designed to split the system in two counterpropagating halves. After a short dephasing period the atoms continued to collide repeatedly for hundreds of times without thermalizing, as in the case of a three-dimensional system. Such long-lived nonthermal states are called prethermal, and they are a consequence of the near integrability of the system under consideration. Recent realizations of similar or slightly modified setups involving dipolar dysprosium atoms were reported in [109,110]. Theoretical and numerical investigations of impenetrable bosons in the QNC setup using the quench action [111,112] and the numerical method presented in Sec. VB were previously performed both at zero [102] and finite temperature [97]. A comprehensive numerical treatment of the finite coupling case using the generalized hydrodynamics [113,114] can be found in [115] (see also [116]).

For the modeling of the Bragg pulse, which initiates the oscillation, we are going to use the results of [31,102]. In the notation and terminology of the latter reference we are going to consider the case of the so-called Kapitza-Dirac pulse, which can be described by the operator ($\hbar = k_B = 1$)

$$U(q, A) = \exp\left(-iA \int \cos(qz) \Psi^\dagger(z) \Psi(z) dz\right). \quad (38)$$

For any state of the system $|\psi\rangle$ the effect of this instantaneous pulse is to produce a new state $|\psi_{q,A}\rangle = U(q, A)|\psi\rangle$. In typical experiments $A \sim 1$ and $q \sim 2\pi n$ with n the density. The long-pulse Bragg regime can be modeled as in [97] by adding to

the harmonic potential a periodic lattice potential $V_B(z, t) = \Omega(t) \cos(2qz)$, with $\Omega(t)$ a sequence of two square pulses.

The evolution of the system after the Bragg pulse is driven by the Hamiltonian (5) with $g = \infty$. The dual fermionic system describes free fermions in a harmonic potential $V(z, t) = m\omega^2 z^2/2$ for which the single-particle wave functions are the well-known Hermite functions

$$\phi_j(z) = e^{-m\omega^2 z^2/2} \frac{1}{\sqrt{2^j j!}} \left(\frac{m\omega}{\pi}\right)^{1/4} H_j(\sqrt{m\omega} z), \quad (39)$$

with $H_j(z)$ denoting the Hermite polynomials and $E_j = \omega(j + 1/2)$. The harmonic oscillator length is $l_{ho} = \sqrt{1/m\omega}$. The action of the Bragg pulse (38) on the SP wave functions is given by $U(q, A)\phi_j(z) = e^{-iA \cos(qz)} \phi_j(z)$. The time-evolved wave functions can be determined using the propagator of the quantum harmonic oscillator [102]

$$\phi_j(z, t) = \int_{-\infty}^{+\infty} K(z, u|t) e^{-iA \cos(qu)} \phi_j(u) du, \quad (40)$$

with (see 2.5.18 of [117])

$$K(z, u|t) = \left(\frac{m\omega}{2\pi i \sin(\omega t)}\right)^{1/2} \times \exp\left(\frac{-m\omega(z^2 + u^2) \cos(\omega t) + 2m\omega zu}{2i \sin(\omega t)}\right). \quad (41)$$

Using the Jacobi-Anger expansion $e^{z \cos \theta} = I_0(z) + 2 \sum_{k=1}^{\infty} I_k(z) \cos k\theta$ (9.6.34 of [118]) with $I_k(z) = \int_0^\pi e^{z \cos \theta} \cos(k\theta) d\theta / \pi$ the modified Bessel function of the first kind in the form $e^{-iz \cos \theta} = \sum_{k=-\infty}^{\infty} I_k(-iz) e^{-ik\theta}$ and the identity (7.374(8) of [119])

$$\int_{-\infty}^{+\infty} e^{-(u-z)^2} H_j(\alpha u) du = \sqrt{\pi} (1 - \alpha^2)^{j/2} H_j\left(\frac{\alpha z}{\sqrt{1 - \alpha^2}}\right),$$

we find [102]

$$\phi_j(z, t) = \sum_{n=-\infty}^{\infty} I_n(-iA) e^{-inq \cos(\omega t)(z + n \frac{q \sin(\omega t)}{2m\omega})} \times \phi_j\left(z + n \frac{q \sin(\omega t)}{m\omega}\right) e^{-i\omega(j + \frac{1}{2})t}. \quad (42)$$

The wave functions are periodic in time with period $T = 2\pi/\omega$, and at first impression it would seem that also the real-space density and one-particle density matrix have the same periodicity. However, using the fact that $I_n(-iA) = I_{-n}(-iA)$, it is easy to see that

$$\phi_j\left(z, t + \frac{\pi}{\omega}\right) = e^{-i(j + \frac{1}{2})\pi} \phi_j(z, t), \quad (43)$$

which implies that all the n -particle reduced matrices are in fact periodic with period $T = \pi/\omega$. This is due to the fact that in their definition (12) the wave functions appear in the form $\psi_{N,A,\nu} \psi_{N,A,\nu}^*$, and from the Anyon-Fermi mapping (7) we have

$$\psi_{N,A,\nu}\left(\mathbf{z} \left| t + \frac{\pi}{\omega} \right.\right) = A(\mathbf{z}) B(\mathbf{z}) e^{-i \sum \nu_j (v_j + \frac{1}{2}) \pi} \psi_{N,F,\nu}(\mathbf{z} | t).$$

Therefore it will be sufficient to study the dynamics of the real-space density and momentum distribution for $t \in [0, \pi/\omega]$. We should point out that this periodicity is particular

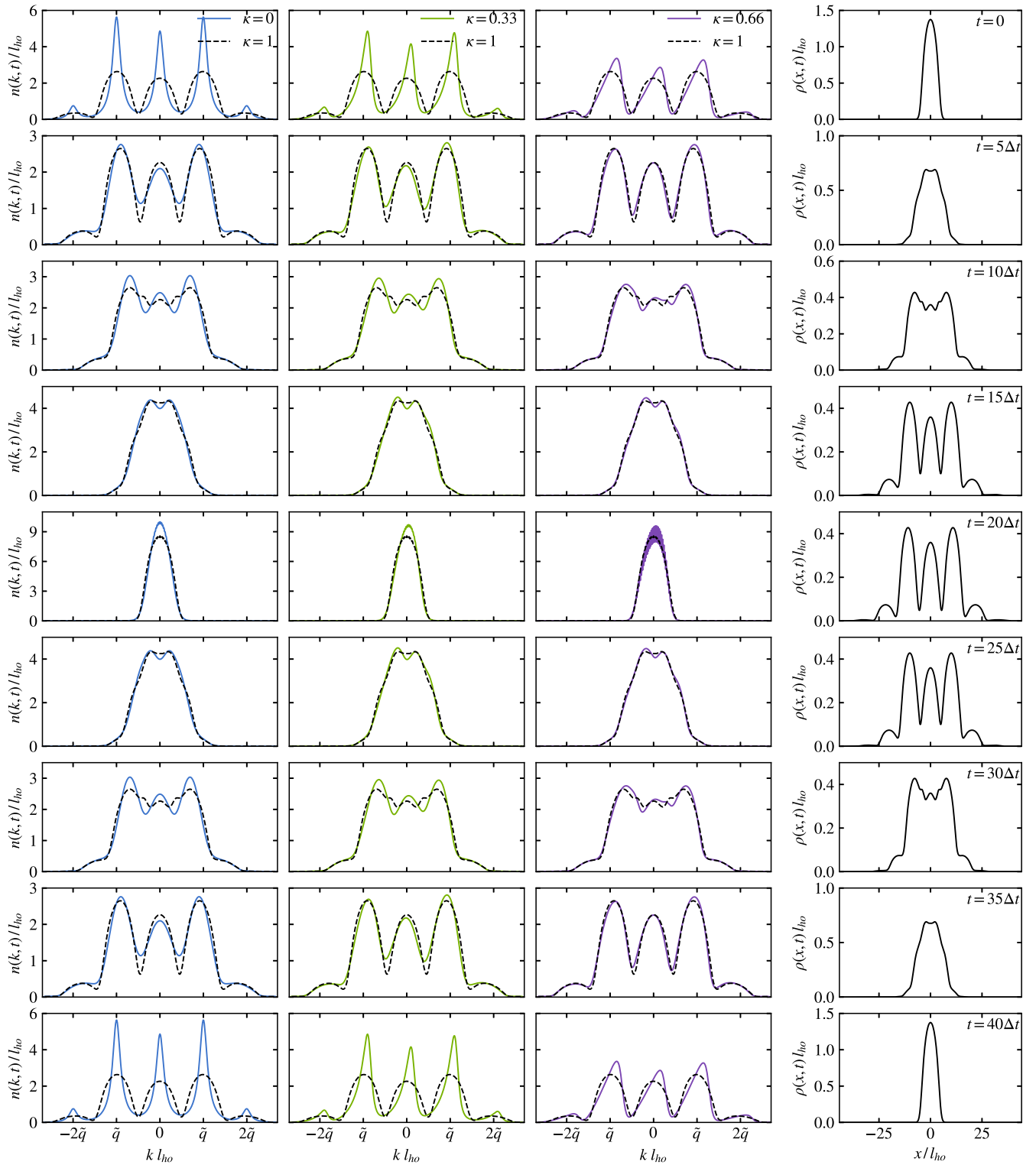


FIG. 1. Dynamics of the momentum distribution of impenetrable anyons ($\kappa = 0$ first column, $\kappa = 0.33$ second column, and $\kappa = 0.66$ third column) and free fermions ($\kappa = 1$) in the QNC setup. The last column presents the dynamics of the real-space density, which is independent of statistics. Here $N = 10$, $A = 1.5$, $ql_{ho} = 10.73$ ($q = 6\pi$, $l_{ho} = 0.57$, $\omega = 3$), and the initial dimensionless temperature is $\theta_0 = 0.083$ ($T_0 = 0.25$). The time step is $\Delta t = \pi/(40\omega)$ and $\tilde{q} = ql_{ho}$.

to the TG regime and is no longer valid in the case of finite coupling.

It will be useful to introduce a dimensionless initial temperature defined by $\theta_0 = T_0/N\omega$. In Fig. 1 we present

the dynamics of the momentum distribution and real-space density in the QNC setup for $N = 10$ anyons at initial dimensionless temperature $\theta_0 = 0.083$ with $A = 1.5$ and $q = 6\pi$ the parameters of the Bragg pulse. In the first three columns

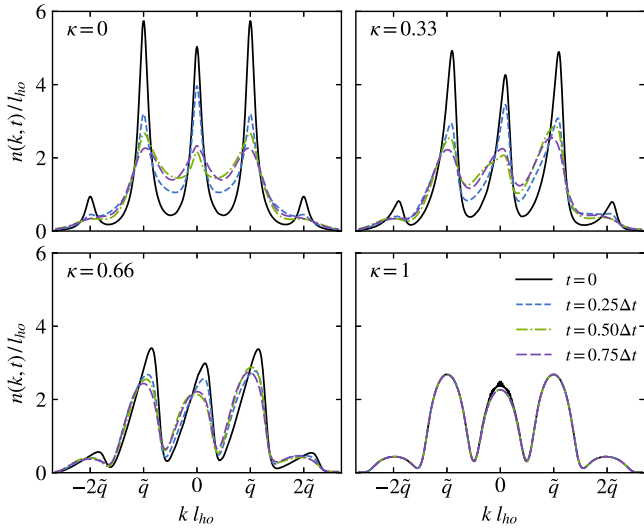


FIG. 2. Evolution of the momentum distribution immediately after the pulse in the QNC setup. The parameters of the system are the same as in Fig. 1.

we plot the momentum distributions of impenetrable bosons ($\kappa = 0$) and anyons with $\kappa = 0.33$ and $\kappa = 0.66$ together with the momentum distribution of free fermions ($\kappa = 1$). For all values of the statistics parameter the evolution during a period is similar: immediately after the Bragg pulse the momentum distribution presents local maxima at $\pm q$ and $\pm 2q$ followed by the well-known oscillations. The distinguishing feature of the anyonic particles is the nonsymmetric momentum distribution, which is most visible in the vicinity of $t = p\pi/\omega$ with $p = 0, 1, 2, \dots$. This is a well-known characteristic of 1D anyons [40,44,53,85] and is a result of the broken space-reversal symmetry [see (4) and (2)]. During the evolution we see that for all values of κ the overlap between the momentum distribution of anyons and free fermions becomes significant and reaches its minimum in the vicinity of $t = p\pi/\omega$ with $p = 0, 1, 2, \dots$. In the bosonic case a similar phenomenon was first described in [120] in the context of breathing oscillations, and it was dubbed (periodic) dynamical fermionization. The dynamics of the real-space density is presented in the last column of Fig. 1.

It was discovered in [102] that there are two different timescales in the QNC evolution. In addition to the slow in-trap periodic behavior presented in Fig. 1, the system also exhibits rapid relaxation immediately after the pulse, which is shown in Fig. 2. The amplitude of this relaxation is largest for the bosonic system and monotonically decreases as we increase the statistics parameter, so it can be said that is directly proportional with the degree of “interaction” of the system. In the case of the fermionic system (which is noninteracting) we see that the momentum distribution is almost unchanged immediately after the pulse.

The dependence of relaxed momentum distribution function on the Bragg momentum q and the parameter A can be found in Fig. 3. If A is too small, the Bragg pulse will not remove the majority of particles from the vicinity of $k = 0$ and the periodic oscillations will not be clearly visible. In the bosonic case for $A = 1.5$ the characteristic ghost shape of the

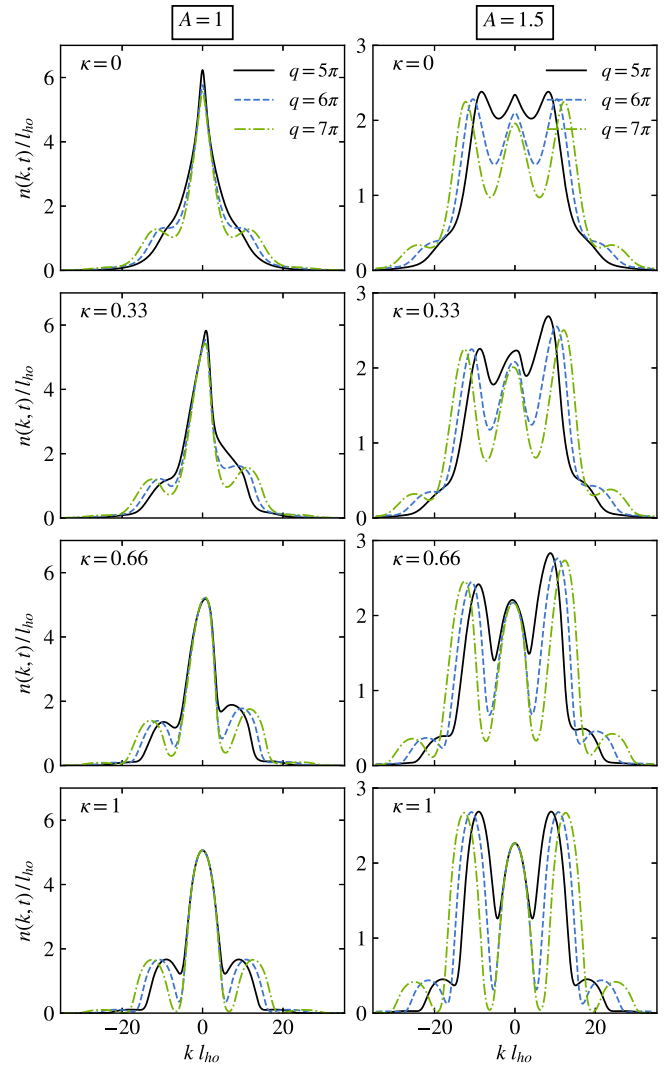


FIG. 3. Dependence of the relaxed momentum distribution function for $N = 10$ particles on the Bragg momentum q and A . In the first column $A = 1$ and in the second column $A = 1.5$. The initial dimensionless temperature is $\theta_0 = 0.083$ ($T_0 = 0.25$), $l_{ho} = 0.57$, $\omega = 3$, and $t = \Delta t$ with $\Delta t = \pi/(40\omega)$.

relaxed momentum distribution is clearly visible and becomes more pronounced with increasing Bragg momentum q . Also, as expected, the width of the momentum distribution is a monotonically increasing function of both q and A . In the case of anyonic particles the relaxed distribution is asymmetric with respect to $k = 0$.

The influence of the initial temperature on the relaxed momentum distribution is shown in Fig. 4. As the initial temperature increases, the $\pm q$ satellites become less and less pronounced and the observation of the oscillations becomes harder.

VII. DYNAMICS IN A HARMONIC TRAP WITH TIME-DEPENDENT FREQUENCY

Another experimentally relevant situation that we are going to investigate is the dynamics of a gas in a harmonic potential with time-dependent frequency $V(z, t) = m\omega^2(t)z^2/2$. We are

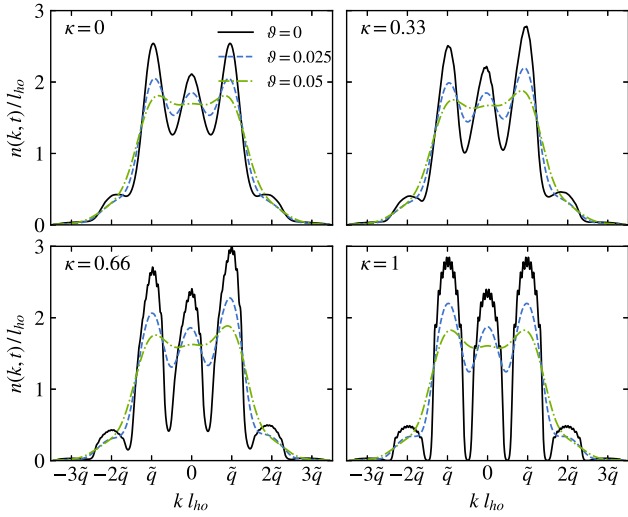


FIG. 4. Dependence on the initial temperature of the relaxed momentum distribution. Here $N = 10$, $A = 1.5$, $q = 6\pi$, $l_{ho} = 0.56$, $\omega = 3$, and $t = 2\Delta t$ with $\Delta t = \pi/(40\omega)$.

going to denote the frequency of the potential at $t = 0$ by ω_0 . At $t = 0$ the SP wave functions are given by (39) with $\omega = \omega_0$. The study of the dynamics in this case is significantly simplified by the fact that the time evolution of the wave functions is given by the following scaling transformation ([121], Chap. VII of [122]):

$$\phi_j(z, t) = \frac{1}{\sqrt{b(t)}} \phi_j\left(\frac{z}{b(t)}, 0\right) e^{i\frac{mz^2}{2} \frac{\dot{b}(t)}{b(t)} - iE_j \tau(t)}, \quad (44)$$

with $b(t)$ the solution of the second-order differential equation $\ddot{b} + \omega^2(t)b = \omega_0^2/b^3$, also known as the Ermakov-Pinney equation, with initial conditions $b(0) = 1$, $\dot{b}(0) = 0$, and $\tau(t) = \int_0^t dt'/b^2(t')$. Equation (44) represents the unique time-dependent solution of the Schrödinger equation $i\hbar\partial\phi_j(z, t)/\partial t = H_{SP}(z, t)\phi_j(z, t)$ with $H_{SP}(z, t) = -(\hbar^2/2m)(\partial^2/\partial z^2) + V(z, t)$, where $H_{SP}(z, 0)\phi_j(z) = \omega_0(j + 1/2)\phi_j(z)$.

Using the formula for the Slater determinant (9) and the fact that the Anyon-Fermi mapping is unchanged by the scaling transformation, the N -body anyonic wave function satisfies

$$\begin{aligned} \psi_{N,A,\nu}(\mathbf{z}|t) &= \frac{1}{b^{N/2}} \psi_{N,A,\nu}(\mathbf{z}/b|0) e^{-i\sum_j E_{\nu_j} \tau} \\ &\times e^{i\frac{\dot{b}}{b} \sum_j m z_j^2 / 2}. \end{aligned} \quad (45)$$

Inserting (45) in the definition of the one-body density matrix (10), we find [120] (see also [123,124])

$$\rho^{(1)}(x, y|t) = \frac{1}{b} \rho^{(1)}\left(\frac{x}{b}, \frac{y}{b} | 0\right) e^{-i\frac{\dot{b}}{b} \frac{m(x^2 - y^2)}{2}}. \quad (46)$$

The momentum distribution function can also be written as (we perform the change of variables $x'/b, y'/b \rightarrow x, y$)

$$n(k, t) = b \int dx dy \rho^{(1)}(x, y|0) e^{-ib[\frac{\dot{b}}{b} \frac{m(x^2 - y^2)}{2} + k(x - y)]}. \quad (47)$$

The simplification introduced by Eq. (46) is now evident. The study of the dynamics is now reduced to the calcula-

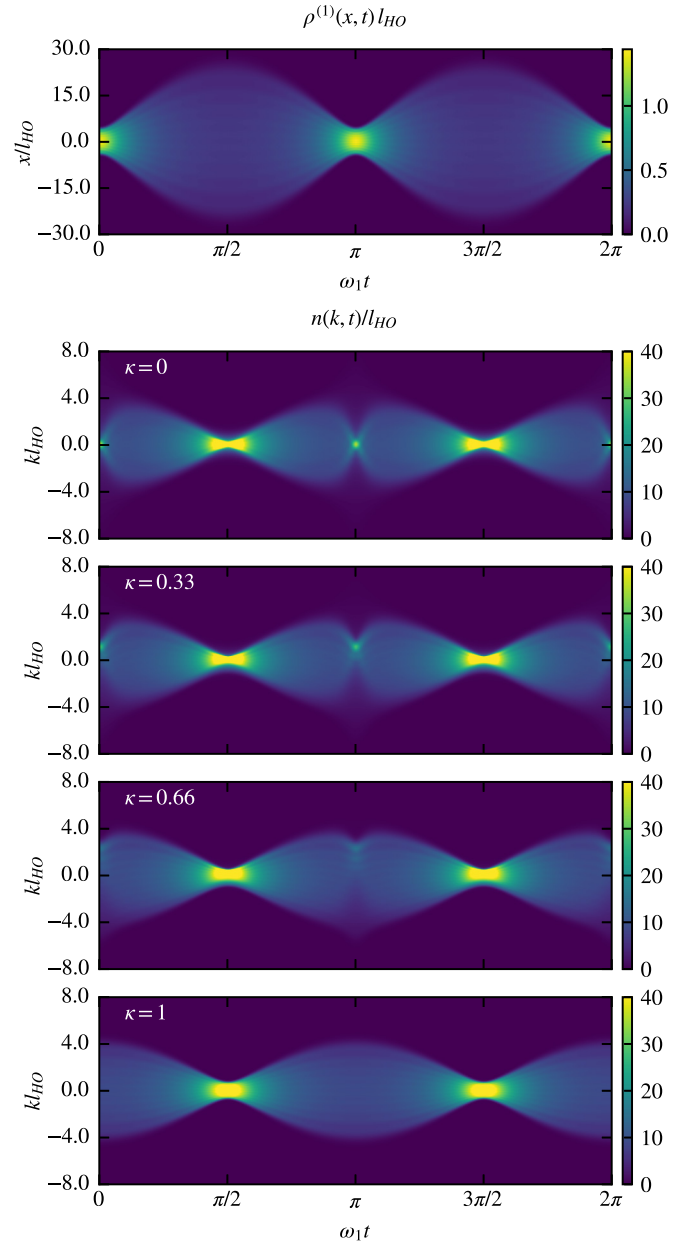


FIG. 5. Evolution of the real-space density (upper panel) and momentum distribution (lower panels) of an anyonic TG gas of $N = 10$ particles after a confinement quench of the frequency with $\epsilon = 35$ and initial dimensionless temperature $\theta_0 = 0.02$ ($T_0 = 1.2$).

tion of the initial ($t = 0$) reduced density matrix at thermal equilibrium supplemented by the solution of the Ermakov-Pinney equation. In this case it is preferable to numerically evaluate the initial RDM using the method of Sec. VB due to the fact that the off-diagonal overlaps can be analytically calculated [125]. Following [97] we introduce $\xi = z/l_{ho}$ and $\varphi_j(\xi) = \sqrt{l_{ho}} \phi_j(z)$. Then for $j \neq k$ we have (formula B.16 of [125])

$$\int \varphi_j(\xi) \varphi_k^*(\xi) d\xi = e^{-\xi^2} \frac{[H_{j+1}(\xi)H_k(\xi) - H_j(\xi)H_{k+1}(\xi)]}{2(k-j)(2^{j+k}\pi j!k!)^{1/2}}. \quad (48)$$

For the diagonal elements it seems that a similar formula does not exist, but an efficient recursive formula can be devised as

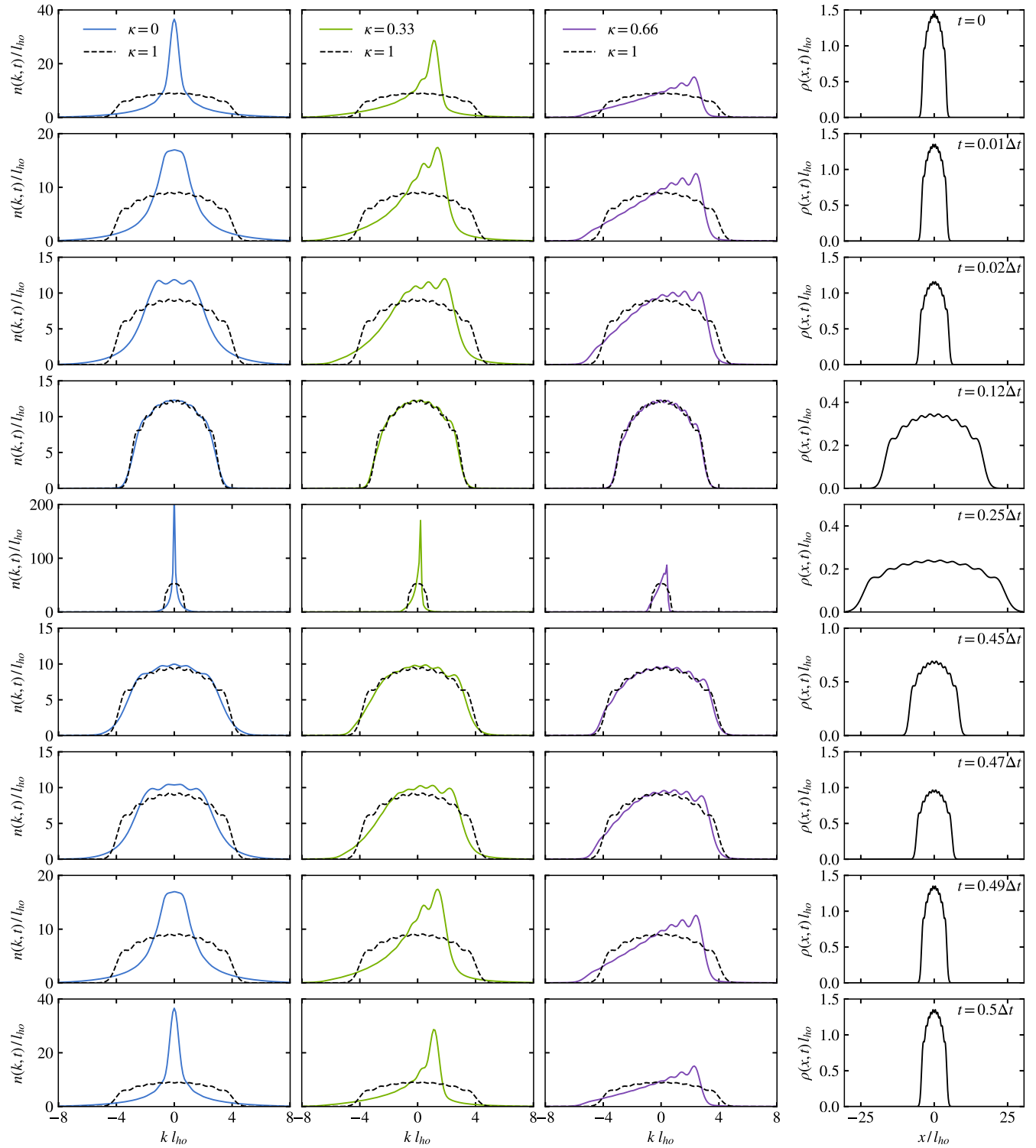


FIG. 6. Momentum distribution (first three columns) and real-space density (last column) of an anyonic TG gas after a confinement quench of the frequency for selected values of t . We use the same parameters as in Fig. 5 and $\Delta t = 2\pi/\omega_1$.

follows [97]. We define a sequence of functions $\{M_j(\xi)\}_{j=0}^{\infty}$ with $M_0(\xi) = 0$ and the general term satisfying

$$M_j(\xi) = \frac{\sqrt{\pi}}{2} \text{erf}(\xi) - \frac{1}{2^j j!} \int e^{-\xi^2} H_j^2(\xi) d\xi, \quad (49)$$

where $\text{erf}(\xi) = 2 \int_0^\xi e^{-t^2} dt / \sqrt{\pi}$ is the error function. Using the recurrence relation for Hermite polynomials $H_{j+1}(\xi) = 2\xi H_j(\xi) - H_j'(\xi)$ we find

$$M_{j+1}(\xi) = M_j(\xi) + \frac{e^{-\xi^2}}{2^{j+1}(j+1)!} H_j(\xi) H_{j+1}(\xi). \quad (50)$$

Using (48), (49), and (50), all the elements of the matrix \mathbf{P} defined in (37) can be calculated analytically without resorting to time-consuming numerical integration.

We are going to consider the situation when initially the gas is in thermal equilibrium at temperature T_0 in the presence of the harmonic potential $V(z) = m\omega_0^2 z^2/2$ and perform an instantaneous change of the trapping frequency from ω_0 to ω_1 at $t = 0$. The quench strength will be parameterized by a dimensionless parameter $\epsilon = \omega_0^2/\omega_1^2 - 1$. For this particular quench the Ermakov-Pinney equation takes the form $\ddot{b} + \omega_1^2 b = \omega_0^2/b^3$ with the solution $b(t) = [1 + \epsilon \sin^2(\omega_1 t)]^{1/2}$, which describes periodic oscillations between 1 and ω_0/ω_1 with period $T = \pi/\omega_1$.

The breathing-mode dynamics of the anyonic TG gas initiated by the quench of the frequency is presented in Fig. 5. While the real-space density displays undamped oscillations with period $T = \pi/\omega_1$, the dynamics of the momentum distribution displays a richer structure. Similar to the case of impenetrable bosons at zero temperature studied in [120] and the QNC case (see the previous section), the momentum distribution of the TG anyonic gas displays alternatively anyonic and fermionic features. This dynamical fermionization occurs rapidly for t close to zero and T , as it can be seen in Fig. 6, where we present the momentum distribution for anyonic gases with $\kappa = \{0, 0.33, 0.66, 1\}$ at selected values of t . The overlap between the anyonic and fermionic momentum distribution is very large for almost the entire period, with the exception of a time interval around $t = T/2$ where the system recovers the initial anyonic distribution rescaled by a factor $b_{\max} > 1$. At zero temperature and for $\kappa = 0$ we have $b_{\max} = \omega_0/\omega_1$ and $n(k, T/2) = b_{\max} n(b_{\max} p, 0)$ [120].

Another interesting feature of the momentum distribution is that it displays narrowing and broadening cycles occurring at twice the rate of the real-space density. This phenomenon was first identified in the bosonic case in [97], further studied in [103], and it can be clearly seen in Fig. 5. While the fermionic system presents narrowing of $n(k, t)$ at $\omega_1 t = \pi/2 + \pi l$ with $l = 1, 2, \dots$, in the anyonic case the momentum distribution presents an additional narrowing at $\omega_1 t = \pi l$ when the gas is maximally compressed. This narrowing is the largest for $\kappa = 0$, and as we increase the statistics parameter

it decreases in an asymmetric (with respect to k) fashion until it disappears for the fermionic system. In [97,103] it was argued that this phenomenon is a collective many-body bounce effect due to the increased thermodynamic pressure of the maximally compressed gas which acts as a potential barrier.

VIII. CONCLUSIONS

In this paper we have derived an exact description of the nonequilibrium dynamics of an anyonic TG gas at finite temperature, generalizing the results of [97]. The evolution of the anyonic one-particle RDM after a quantum quench from an initial thermal state is given by the Fredholm minor of an integral operator, with the kernel being the thermal RDM of free fermions. The statistics parameter enters in the constant in front of the integral operator. We have argued that when the overlaps of the evolved wave functions cannot be calculated analytically, the most efficient numerical evaluation of the RDM is based on Nyström’s method of solving Fredholm integral equations of the second kind. We have investigated the nonequilibrium dynamics of the anyonic TG gas in two experimental relevant scenarios: the QNC and the breathing oscillations initiated by a sudden quench of the trapping frequency. A natural extension of our work would be to investigate the finite-temperature dynamics of the bipartite entanglement, as it was already noticed in [126] that Nyström’s method is more efficient in computing the entanglement entropy in situations in which the overlap matrix cannot be computed analytically. Other promising avenues of research are the investigation of the anyonic spectral function [127], the entanglement revival [128], or the nonequilibrium quantum thermodynamics [129]. This will be deferred to future publications.

ACKNOWLEDGMENTS

Financial support from the LAPLAS 6 program of the Romanian National Authority for Scientific Research (CNCS-UEFISCDI) is gratefully acknowledged.

APPENDIX A: FREDHOLM MINORS

In this Appendix we present some basic definitions and useful formulas involving Fredholm minors which were used in the main text. Consider a Fredholm integral equation of the second kind (for more information on Fredholm integral equation see Chap. II of [130] or Chap. I of [131]),

$$g(\lambda) = f(\lambda) + \gamma \int_{\Omega} \mathbf{K}(\lambda, \mu) g(\mu) d\mu, \tag{A1}$$

where $f(\lambda)$ is a continuous complex function defined on the bounded set Ω , and the kernel $\mathbf{K}(\lambda, \mu)$ is a continuous complex function of λ and μ on $\Omega \times \Omega$. The set $\hat{\Omega}$ may be a bounded interval or the reunion of a finite number of such intervals. The n th Fredholm minor of the integral operator $\hat{\mathbf{K}}$ is given by the series

$$D_n \left(\begin{matrix} \lambda_1 & \cdots & \lambda_n \\ \mu_1 & \cdots & \mu_n \end{matrix} \middle| \gamma \right) = \mathbf{K} \left(\begin{matrix} \lambda_1 & \cdots & \lambda_n \\ \mu_1 & \cdots & \mu_n \end{matrix} \right) + \sum_{p=1}^{\infty} \frac{(-\gamma)^p}{p!} \int_{\Omega} \cdots \int_{\Omega} \mathbf{K} \left(\begin{matrix} \lambda_1 & \cdots & \lambda_n & v_1 & \cdots & v_p \\ \mu_1 & \cdots & \mu_n & v_1 & \cdots & v_p \end{matrix} \right) dv_1 \cdots dv_p, \tag{A2}$$

where we have introduced the notation

$$\mathbf{K} \begin{pmatrix} \lambda_1 & \cdots & \lambda_n \\ \mu_1 & \cdots & \mu_n \end{pmatrix} = \begin{vmatrix} \mathbf{K}(\lambda_1, \mu_1) & \mathbf{K}(\lambda_1, \mu_2) & \cdots & \mathbf{K}(\lambda_1, \mu_n) \\ \mathbf{K}(\lambda_2, \mu_1) & \mathbf{K}(\lambda_2, \mu_2) & \cdots & \mathbf{K}(\lambda_2, \mu_n) \\ \vdots & \vdots & \ddots & \vdots \\ \mathbf{K}(\lambda_n, \mu_1) & \mathbf{K}(\lambda_n, \mu_2) & \cdots & \mathbf{K}(\lambda_n, \mu_n) \end{vmatrix}. \quad (\text{A3})$$

The series (A2) converges for all values of the parameter γ , and D_n is antisymmetric in both λ_i 's and μ_i 's by construction. Particular cases of the series which will play an important role in our analysis are the $n = 0$ case known as the Fredholm determinant

$$D(\gamma) \equiv \det(1 - \gamma \hat{\mathbf{K}}) = 1 + \sum_{p=1}^{\infty} \frac{(-\gamma)^p}{p!} \int_{\Omega} \cdots \int_{\Omega} \mathbf{K} \begin{pmatrix} \nu_1 & \cdots & \nu_p \\ \nu_1 & \cdots & \nu_p \end{pmatrix} d\nu_1 \cdots d\nu_p, \quad (\text{A4})$$

and the first minor ($n = 1$)

$$D \left(\begin{matrix} \lambda \\ \mu \end{matrix} \middle| \gamma \right) = \mathbf{K}(\lambda, \mu) + \sum_{p=1}^{\infty} \frac{(-\gamma)^p}{p!} \int_{\Omega} \cdots \int_{\Omega} \mathbf{K} \begin{pmatrix} \lambda & \nu_1 & \cdots & \nu_p \\ \mu & \nu_1 & \cdots & \nu_p \end{pmatrix} d\nu_1 \cdots d\nu_p. \quad (\text{A5})$$

If $D(\gamma) \neq 0$, a solution of the integral equation (A1) is given by

$$g(\lambda) = f(\lambda) + \gamma \int_{\Omega} \mathbf{R}(\lambda, \mu) f(\mu) d\mu, \quad (\text{A6})$$

with the function $\mathbf{R}(\lambda, \mu)$ called the resolvent kernel, which satisfies

$$\mathbf{R}(\lambda, \mu) = \mathbf{K}(\lambda, \mu) + \gamma \int_{\Omega} \mathbf{K}(\lambda, \nu) \mathbf{R}(\nu, \mu) d\nu \quad (\text{A7})$$

and is given by

$$\mathbf{R}(\lambda, \mu) = D \left(\begin{matrix} \lambda \\ \mu \end{matrix} \middle| \gamma \right) / \det(1 - \gamma \hat{\mathbf{K}}). \quad (\text{A8})$$

Formula (A8) is a particular case of a more general identity first proved by Hurwitz [132] and possibly rediscovered many times [133], which relates the n th minor to the resolvent kernel

$$D_n \begin{pmatrix} \lambda_1 & \cdots & \lambda_n \\ \mu_1 & \cdots & \mu_n \end{pmatrix} \middle| \gamma = \det(1 - \gamma \hat{\mathbf{K}}) \mathbf{R} \begin{pmatrix} \lambda_1 & \cdots & \lambda_n \\ \mu_1 & \cdots & \mu_n \end{pmatrix}. \quad (\text{A9})$$

APPENDIX B: REDUCED DENSITY MATRICES FOR FREE FERMIONS

Here we compute the n -body RDMs for free fermions in a time-dependent confining potential following Lenard [99]. Using the symmetry of the fermionic wave functions, we see that an alternative definition for the fermionic RDMs is given by

$$\rho_F^{(n)}(\mathbf{x}, \mathbf{y} | t) = \sum_{N=n}^{\infty} \sum_{\mathbf{v}} p(N, \mathbf{v}) \frac{N!}{(N-n)!} \int dz_{n+1} \cdots dz_N \psi_{N,F,\mathbf{v}}(\mathbf{x}, \tilde{\mathbf{z}} | t) \psi_{N,F,\mathbf{v}}^*(\mathbf{y}, \tilde{\mathbf{z}} | t), \quad (\text{B1})$$

with $\mathbf{x} = (x_1, \dots, x_n)$, $\mathbf{y} = (y_1, \dots, y_n)$, and $\tilde{\mathbf{z}} = (z_{n+1}, \dots, z_N)$. The wave functions are given by the Slater determinants (9), and we are going to consider the grand-canonical ensemble with $p(N, \mathbf{v}) = e^{-(E_{N,\mathbf{v}} - \mu N)/k_B T_0} / \mathcal{Z}$.

As a starting point we will derive a preliminary result. Consider

$$G = \sum_{\mathbf{v}} e^{-(E_{N,\mathbf{v}} - \mu N)/k_B T_0} \psi_{N,F,\mathbf{v}}(x_1, \dots, x_N | t) \psi_{N,F,\mathbf{v}}^*(y_1, \dots, y_N | t). \quad (\text{B2})$$

The summand is symmetric in ν_i 's and vanishes when two of them are equal, which means that G can be written as

$$G = \frac{1}{N!} \sum_{\nu_1} \cdots \sum_{\nu_N} e^{-(\sum_i E_{\nu_i} - \mu N)/k_B T_0} \psi_{N,F,\mathbf{v}}(x_1, \dots, x_N | t) \psi_{N,F,\mathbf{v}}^*(y_1, \dots, y_N | t). \quad (\text{B3})$$

Using the sum over the permutations form of the determinant, we find

$$\begin{aligned} G &= \frac{1}{(N!)^2} \sum_{\nu_1} \cdots \sum_{\nu_N} \left(\prod_{j=1}^N e^{-(E_{\nu_j} - \mu N)/k_B T_0} \right) \left(\sum_{P \in S_N} (-1)^P \prod_{j=1}^N \phi_{\nu_j}(x_{P(j)}, t) \right) \left(\sum_{Q \in S_N} (-1)^Q \prod_{j=1}^N \phi_{\nu_j}^*(y_{Q(j)}, t) \right), \\ &= \frac{1}{(N!)^2} \sum_{\nu_1} \cdots \sum_{\nu_N} \left(\prod_{j=1}^N e^{-(E_{\nu_j} - \mu N)/k_B T_0} \right) \sum_{P \in S_N} \sum_{R \in S_N} (-1)^R \prod_{j=1}^N \phi_{\nu_j}(x_{P(j)}, t) \phi_{\nu_j}^*(y_{R(j)}, t), \end{aligned}$$

$$\begin{aligned}
 &= \frac{1}{(N!)^2} \sum_{P \in S_N} \sum_{R \in S_N} (-1)^R \prod_{j=1}^N \sum_{\nu_j} e^{-(E_{\nu_j} - \mu N)/k_B T_0} \phi_{\nu_j}(x_{P(j)}, t) \phi_{\nu_j}^*(y_{RP(j)}, t), \\
 &= \frac{1}{N!} \mathbf{f} \begin{pmatrix} x_1 & \cdots & x_N \\ y_1 & \cdots & y_N \end{pmatrix}; t, \quad \mathbf{f}(x, y|t) = \sum_{\nu} e^{-(E_{\nu} - \mu N)/k_B T_0} \phi_{\nu}(x, t) \phi_{\nu}^*(y, t),
 \end{aligned} \tag{B4}$$

where S_N is the group of permutations of N elements, $(-1)^P$ is the signature of the permutation P , and in the second line we have used the fact that every permutation Q can be written as $Q = RP$ with signature $(-1)^{R+P}$. In a similar fashion we can compute the grand-canonical partition function as

$$\begin{aligned}
 \mathcal{Z} &= \sum_{N=0}^{\infty} \sum_{\nu} e^{-(E_{N,\nu} - \mu N)/k_B T_0} = \sum_{N=0}^{\infty} \sum_{\nu} e^{-(E_{N,\nu} - \mu N)/k_B T_0} \int dz_1 \cdots \int dz_N |\psi_{N,F,\nu}(z_1, \dots, z_N)|^2, \\
 &= \sum_{N=0}^{\infty} \frac{1}{N!} \int dz_1 \cdots \int dz_N \mathbf{f} \begin{pmatrix} x_1 & \cdots & x_N \\ y_1 & \cdots & y_N \end{pmatrix}; t = \det(1 + \hat{\mathbf{f}}),
 \end{aligned} \tag{B5}$$

which shows that the partition function can be expressed as the Fredholm determinant of an integral operator with kernel $\mathbf{f}(x, y|t)$. Inserting $p(N, \nu) = e^{-(E_{N,\nu} - \mu N)/T} / \mathcal{Z}$ in Eq. (B1), we find $\rho_F^{(n)}(x, y|t) = H/\mathcal{Z}$, where

$$\begin{aligned}
 H &= \sum_{N=n}^{\infty} \sum_{\nu} e^{-(E_{N,\nu} - \mu N)/k_B T_0} \frac{N!}{(N-n)!} \int dz_{n+1} \cdots \int dz_N \psi_{N,F,\nu}(\mathbf{x}, \tilde{\mathbf{z}}, |t) \psi_{N,F,\nu}^*(\mathbf{y}, \tilde{\mathbf{z}}, |t), \\
 &= \sum_{N=n}^{\infty} \frac{1}{(N-n)!} \int dz_{n+1} \cdots \int dz_N \mathbf{f} \begin{pmatrix} x_1 & \cdots & x_n & z_{n+1} & \cdots & z_N \\ y_1 & \cdots & y_n & z_{n+1} & \cdots & z_N \end{pmatrix}; t, \\
 &= D_n \left(\begin{matrix} x_1 & \cdots & x_n \\ y_1 & \cdots & y_n \end{matrix} \middle| -1 \right),
 \end{aligned} \tag{B6}$$

which shows that H is the n th Fredholm minor of the integral operator with kernel $\mathbf{f}(x, y|t)$ and $\gamma = -1$ [see (A2)]. Collecting (B5) and (B6) and plugging in the definition (B1) we find

$$\rho_F^{(n)}(\mathbf{x}, \mathbf{y}|t) = D_n \left(\begin{matrix} x_1 & \cdots & x_n \\ y_1 & \cdots & y_n \end{matrix} \middle| -1 \right) / \det(1 + \hat{\mathbf{f}}). \tag{B7}$$

We can further simplify this expression by considering the resolvent kernel associated to the integral operator $1 + \hat{\mathbf{f}}$, which will be denoted by $F(\lambda, \mu|t)$ and satisfies the integral equation

$$F(\lambda, \mu|t) + \int \mathbf{f}(\lambda, \nu|t) F(\nu, \mu|t) d\nu = \mathbf{f}(\lambda, \mu|t). \tag{B8}$$

Expanding $F(\lambda, \mu|t)$ in the orthonormal system $\phi_i(\lambda, t) \phi_i^*(\mu, t)$ we obtain

$$F(\lambda, \mu|t) = \sum_{i=0}^{\infty} \frac{1}{1 + e^{(E_i - \mu)/k_B T_0}} \phi_i(\lambda, t) \phi_i^*(\mu, t), \tag{B9}$$

which shows that $F(\lambda, \mu|t)$ is in fact $\rho_F^{(1)}(x, y|t)$, the one-body RDM of free fermions. From (B7) and Hurwitz's identity (A9) we obtain the final expression for the n -body reduced density matrices of free fermions,

$$\rho_F^{(n)}(\mathbf{x}, \mathbf{y}|t) = \rho_F^{(1)} \begin{pmatrix} x_1 & \cdots & x_n \\ y_1 & \cdots & y_n \end{pmatrix}; t, \tag{B10}$$

with $\rho_F^{(1)}(\lambda, \mu|t) = F(\lambda, \mu|t)$ defined in (B9). For a recent utilization of (B7) and Lenard's formula for $n = 2$ in the context of the full counting statistics of the bosonic Tonks-Girardeau gas see [134].

APPENDIX C: TWO THEOREMS ON GRAM DETERMINANTS

Here we state and prove two theorems on Gram determinants which are useful in deriving the identity (30), which establishes the equivalence in the truncated basis of the Fredholm determinant with the determinant of the overlaps.

Theorem 1. Let $\mathbf{a}_1, \dots, \mathbf{a}_n$ be n linearly independent vectors in an M -dimensional space with $\mathbf{a}_i = (a_{i1}, \dots, a_{iM})$ and the scalar product $\mathbf{a}_i \cdot \mathbf{a}_j = \sum_{k=1}^M a_{ik} a_{jk}^*$ (the star denotes complex conjugation). Then the Gram determinant of the vectors $\mathbf{a}_1, \dots, \mathbf{a}_n$

defined by

$$\Gamma = \begin{vmatrix} \mathbf{a}_1^2 & \mathbf{a}_1 \cdot \mathbf{a}_2 & \cdots & \mathbf{a}_1 \cdot \mathbf{a}_n \\ \mathbf{a}_2 \cdot \mathbf{a}_1 & \mathbf{a}_2^2 & \cdots & \mathbf{a}_2 \cdot \mathbf{a}_n \\ \vdots & \vdots & \ddots & \vdots \\ \mathbf{a}_n \cdot \mathbf{a}_1 & \mathbf{a}_n \cdot \mathbf{a}_2 & \cdots & \mathbf{a}_n^2 \end{vmatrix} \tag{C1}$$

can be expressed as

$$\Gamma = \sum_{1 \leq k_1 < \cdots < k_n \leq M} \begin{vmatrix} a_{1k_1} & a_{1k_2} & \cdots & a_{1k_n} \\ a_{2k_1} & a_{2k_2} & \cdots & a_{2k_n} \\ \vdots & \vdots & \ddots & \vdots \\ a_{nk_1} & a_{nk_2} & \cdots & a_{nk_n} \end{vmatrix}^2, \tag{C2a}$$

$$= \frac{1}{n!} \sum_{k_1=1}^M \cdots \sum_{k_n=1}^M \begin{vmatrix} a_{1k_1} & a_{1k_2} & \cdots & a_{1k_n} \\ a_{2k_1} & a_{2k_2} & \cdots & a_{2k_n} \\ \vdots & \vdots & \ddots & \vdots \\ a_{nk_1} & a_{nk_2} & \cdots & a_{nk_n} \end{vmatrix}^2, \tag{C2b}$$

where $|A|^2 = |A||A^*|$ for any matrix A .

Proof. Using the linearity of the determinant with respect to columns we have

$$\begin{aligned} \Gamma &= \begin{vmatrix} \sum_{k_1=1}^M a_{1k_1} a_{1k_1}^* & \mathbf{a}_1 \cdot \mathbf{a}_2 & \cdots & \mathbf{a}_1 \cdot \mathbf{a}_n \\ \sum_{k_1=1}^M a_{2k_1} a_{1k_1}^* & \mathbf{a}_2^2 & \cdots & \mathbf{a}_2 \cdot \mathbf{a}_n \\ \vdots & \vdots & \ddots & \vdots \\ \sum_{k_1=1}^M a_{nk_1} a_{1k_1}^* & \mathbf{a}_n \cdot \mathbf{a}_2 & \cdots & \mathbf{a}_n^2 \end{vmatrix}, \\ &= \sum_{k_1=1}^M a_{1k_1}^* \begin{vmatrix} a_{1k_1} & \mathbf{a}_1 \cdot \mathbf{a}_2 & \cdots & \mathbf{a}_1 \cdot \mathbf{a}_n \\ a_{2k_1} & \mathbf{a}_2^2 & \cdots & \mathbf{a}_2 \cdot \mathbf{a}_n \\ \vdots & \vdots & \ddots & \vdots \\ a_{nk_1} & \mathbf{a}_n \cdot \mathbf{a}_2 & \cdots & \mathbf{a}_n^2 \end{vmatrix}, \\ &= \sum_{k_1=1}^M \cdots \sum_{k_n=1}^M a_{1k_1}^* a_{2k_2}^* \cdots a_{nk_n}^* \begin{vmatrix} a_{1k_1} & a_{1k_2} & \cdots & a_{1k_n} \\ a_{2k_1} & a_{2k_2} & \cdots & a_{2k_n} \\ \vdots & \vdots & \ddots & \vdots \\ a_{nk_1} & a_{nk_2} & \cdots & a_{nk_n} \end{vmatrix}. \end{aligned} \tag{C3}$$

From the last relation we can see that when two k 's are equal the summand vanishes, which means that we have

$$\begin{aligned} \Gamma &= \sum_{1 \leq k_1 \cdots k_n \leq M} \sum_{P \in S_N} a_{1k_{P(1)}}^* a_{2k_{P(2)}}^* \cdots a_{nk_{P(n)}}^* \begin{vmatrix} a_{1k_{P(1)}} & a_{1k_{P(2)}} & \cdots & a_{1k_{P(n)}} \\ a_{2k_{P(1)}} & a_{2k_{P(2)}} & \cdots & a_{2k_{P(n)}} \\ \vdots & \vdots & \ddots & \vdots \\ a_{nk_{P(1)}} & a_{nk_{P(2)}} & \cdots & a_{nk_{P(n)}} \end{vmatrix}, \\ &= \sum_{1 \leq k_1 \cdots k_n \leq M} \left(\sum_{P \in S_N} (-1)^P a_{1k_{P(1)}}^* a_{2k_{P(2)}}^* \cdots a_{nk_{P(n)}}^* \right) \begin{vmatrix} a_{1k_1} & a_{1k_2} & \cdots & a_{1k_n} \\ a_{2k_1} & a_{2k_2} & \cdots & a_{2k_n} \\ \vdots & \vdots & \ddots & \vdots \\ a_{nk_1} & a_{nk_2} & \cdots & a_{nk_n} \end{vmatrix}, \\ &= \sum_{1 \leq k_1 < \cdots < k_n \leq M} \begin{vmatrix} a_{1k_1} & a_{1k_2} & \cdots & a_{1k_n} \\ a_{2k_1} & a_{2k_2} & \cdots & a_{2k_n} \\ \vdots & \vdots & \ddots & \vdots \\ a_{nk_1} & a_{nk_2} & \cdots & a_{nk_n} \end{vmatrix}^2, \end{aligned} \tag{C4}$$

which proves (C2a). Then (C2b) follows from the fact that the square modulus of the determinant is a symmetric function in k 's and vanishes when two of them are equal.

Theorem 2. Let $\phi_1(x), \dots, \phi_n(x)$ linear independent functions defined on the interval $[a, b]$. Then

$$\begin{aligned} \Gamma &= \left| \int_a^b \phi_i(x) \phi_k^*(x) dx \right|, \\ &= \frac{1}{n!} \int_a^b dx_1 \cdots \int_a^b dx_n \begin{vmatrix} \phi_1(x_1) & \phi_1(x_2) & \cdots & \phi_1(x_n) \\ \phi_2(x_1) & \phi_2(x_2) & \cdots & \phi_2(x_n) \\ \vdots & \vdots & \ddots & \vdots \\ \phi_n(x_1) & \phi_n(x_2) & \cdots & \phi_n(x_n) \end{vmatrix}^2. \end{aligned} \tag{C5}$$

Proof. The Gram determinant can also be written as

$$\begin{aligned} \Gamma &= \int_a^b dx_1 \cdots \int_a^b dx_n \begin{vmatrix} \phi_1(x_1)\phi_1^*(x_1) & \phi_1(x_2)\phi_2^*(x_2) & \cdots & \phi_1(x_n)\phi_n^*(x_n) \\ \phi_2(x_1)\phi_1^*(x_1) & \phi_2(x_2)\phi_2^*(x_2) & \cdots & \phi_2(x_n)\phi_n^*(x_n) \\ \vdots & \vdots & \ddots & \vdots \\ \phi_n(x_1)\phi_1^*(x_1) & \phi_n(x_2)\phi_2^*(x_2) & \cdots & \phi_n(x_n)\phi_n^*(x_n) \end{vmatrix}, \\ &= \int_a^b dx_1 \cdots \int_a^b dx_n \phi_1^*(x_1) \cdots \phi_n^*(x_n) \begin{vmatrix} \phi_1(x_1) & \phi_1(x_2) & \cdots & \phi_1(x_n) \\ \phi_2(x_1) & \phi_2(x_2) & \cdots & \phi_2(x_n) \\ \vdots & \vdots & \ddots & \vdots \\ \phi_n(x_1) & \phi_n(x_2) & \cdots & \phi_n(x_n) \end{vmatrix}, \end{aligned}$$

due to the fact that in the first determinant the integration variable x_j appears only in the j th column. In the last relation we can see that the right-hand side is unchanged if we permute the integration variable. Then we can write

$$\begin{aligned} \Gamma &= \frac{1}{n!} \int_a^b dx_1 \cdots \int_a^b dx_n \sum_{P \in S_N} \phi_1^*(x_{P(1)}) \cdots \phi_n^*(x_{P(n)}) \begin{vmatrix} \phi_1(x_{P(1)}) & \phi_1(x_{P(2)}) & \cdots & \phi_1(x_{P(n)}) \\ \phi_2(x_{P(1)}) & \phi_2(x_{P(2)}) & \cdots & \phi_2(x_{P(n)}) \\ \vdots & \vdots & \ddots & \vdots \\ \phi_n(x_{P(1)}) & \phi_n(x_{P(2)}) & \cdots & \phi_n(x_{P(n)}) \end{vmatrix} \\ &= \frac{1}{n!} \int_a^b dx_1 \cdots \int_a^b dx_n \left(\sum_{P \in S_N} (-1)^P \phi_1^*(x_{P(1)}) \cdots \phi_n^*(x_{P(n)}) \right) \begin{vmatrix} \phi_1(x_1) & \phi_1(x_2) & \cdots & \phi_1(x_n) \\ \phi_2(x_1) & \phi_2(x_2) & \cdots & \phi_2(x_n) \\ \vdots & \vdots & \ddots & \vdots \\ \phi_n(x_1) & \phi_n(x_2) & \cdots & \phi_n(x_n) \end{vmatrix}, \end{aligned}$$

which proves our theorem. Theorem 2 is also known as Andréief's integration formula [135].

APPENDIX D: COMPARISON OF THE TWO NUMERICAL METHODS

In this Appendix we compare the efficiencies of the two numerical methods presented in Secs. VA and VB, which can be used to compute the reduced density matrices of impenetrable anyons. We consider the case when the overlaps of the wave functions cannot be calculated analytically, as in the QNC setup (see Sec. VI).

Both methods require the knowledge of the SP wave functions, which can be calculated either analytically (in some cases) or numerically, solving the time-dependent Schrödinger equation. In general, the wave functions are highly oscillatory functions, and in order to accurately calculate the RDM they need to be computed on a fine grid in an appropriate chosen domain. If the wave functions need to be evaluated for values different from the grid points we will use interpolation. If we have computed such a sampling of the wave functions on the equidistant grid $X = (x_1, \dots, x_n)$ (n is the number of grid points), then we can very easily obtain a sampling of the free fermionic RDM on $X \times X$ which then can be used for the two-dimensional (2D) interpolation of $\rho_F^{(1)}(x, y|t)$. In order to see this, consider the matrix with elements $A_{ij} = f_i^{1/2} \phi_i(x_j, t)$, where f_i is the Fermi-Dirac function and $i = 0, \dots, M - 1$, $j = 1, \dots, n$. (This is the

$M \times n$ matrix constructed by putting on row i the wave function ϕ_i , evaluated on grid X and multiplied by $f_i^{1/2}$.) Then the $n \times n$ values of $\rho_F^{(1)}(x, y|t)$ for $x, y \in X \times X$ are given by the matrix $A^T A^*$, where A^T is the transposed matrix and A^* is the complex conjugate. We point out that the computation of the free fermionic RDM on the 2D grid from the sampled wave functions can be done very quickly. (Even in the case of the largest grid that we have employed, with $n = 3600$ the construction of the matrices and the matrix product took less than a second on a normal laptop.)

A correct evaluation of the efficiency of the two methods should take into account, in addition to the floating-point operations required in each case, the number of calls required by each method for $\phi_i(x, t)$ or $\rho_F^{(1)}(x, y|t)$, when $x \neq X$ or $x, y \neq X \times X$. This is because while function interpolation is very efficient, it is still time consuming compared with a floating-point operation. On our system the time for a call of an interpolated wave function was $t_\phi \sim [1.5, 2.5] \times 10^{-6}$ s and for an interpolated fermionic RDM $t_\rho \sim [4, 5] \times 10^{-6}$ s.

Analysis of the method based on the overlaps. In general, the most time-consuming component of this method is the computation of the wave-function overlaps. Needless to say, the utilization of a general-purpose adaptive subroutine, while very accurate, would be time consuming. In order to minimize

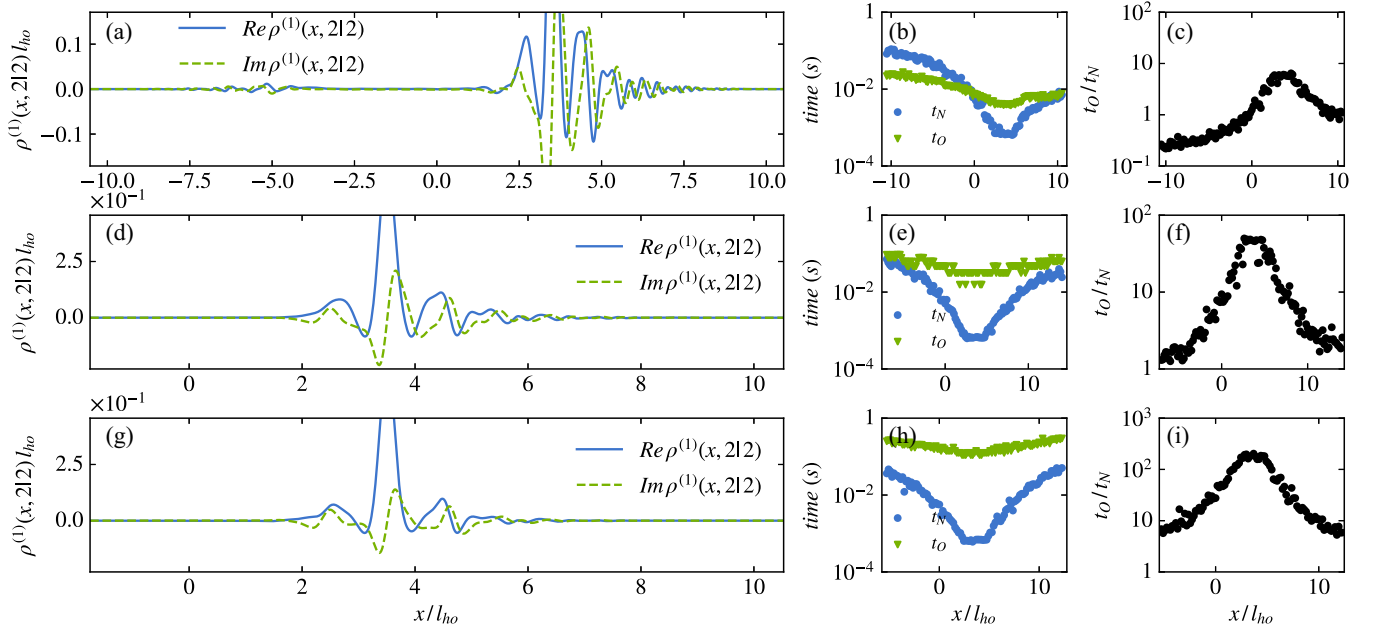


FIG. 7. First column: Real and imaginary part of $\rho^{(1)}(x, y|t)$ for $N = 10$ bosons ($\kappa = 0$ and fixed values of y and t) at different temperatures in the quantum Newton's cradle setting ($l_{ho} = 0.56$, $\omega = 3$, $q = 4\pi$, $A = 1.5$). Here $y = 2$, $t = 2\Delta t$, $\Delta t = \pi/40\omega$, $\theta_0 = 0$ (a), $\theta_0 = 0.011$ (d), and $\theta_0 = 0.025$ (g). Middle column: Evaluation time (logarithmic scale) of the RDM using Nyström's method t_N (disks) and overlaps method t_O (triangles) for the data in the first column. Last column: Plots of the ratios t_O/t_N from the middle column.

the number of calls to the interpolated wave functions, it is preferable to use a quadrature rule whose points and weights can be computed accurately and fast. We have used the Clenshaw-Curtis quadrature, which has a computational cost of $O(p \log_2 p)$, using Waldvogel's FFT algorithm [136] (p is the number of points of the quadrature). It can be argued that a more suitable choice of quadrature would be Gauss-Legendre, but for smooth functions it seems that Clenshaw-Curtis performs as well [137], and our numerical experiments confirm this hypothesis. Using a quadrature with p points, in order to compute the overlaps we need Mp calls of the interpolated wave functions and then $M(M+1)p/2$ multiplications. [Only $M(M+1)/2$ integrals are independent; the rest can be obtained from complex conjugation.] The computation of the inverse and the determinant of \mathbf{P} both require $O(M^3)$ operations; \mathbf{Q} requires M^2 multiplications while the summation in (35) requires $2M$ calls of the interpolated wave functions and M^2 multiplications. Therefore the evaluation time of the truncated basis method for a quadrature with p points and truncation level M is approximately

$$t_O = \left(p \log_2 p + 2M^3 + 2M^2 + \frac{M(M+1)}{2} p \right) t_F + M(p+2)t_\phi, \quad (\text{D1})$$

where t_F is the time required by a floating-point operation.

Analysis of Nyström's method. If we use a quadrature with m points, due to the fact that $\rho^{(1)}(x, y|t) = [\rho^{(1)}(y, x|t)]^*$, the construction of the matrix $\rho^{(1)}(\lambda_i, \lambda_j|t)$ requires $m(m+1)/2$ calls of the interpolated RDM, and the solution of the linear system (22) requires $O(m^3) + O(m^2)$ operations. [The $O(m^2)$ comes from the multiplication of the aforementioned matrix with w_j .] The Fredholm determinant also requires $O(m^3) +$

$O(m^2)$ operations, and the interpolation formula (21) requires $O(m)$ operations and $m+1$ calls of the interpolated RDM. Therefore the approximate evaluation time of Nyström's method is

$$t_N = (m \log_2 m + 2m^3 + 2m^2 + m)t_F + \frac{1}{2}(m+1)(m+2)t_\rho. \quad (\text{D2})$$

Taking into account that $t_\rho \sim 2t_\phi$ and that it is sensible to assume that $p \sim m$ (this was true in all our numerical investigations), from (D1) and (D2) we can already estimate which method is more competitive. Because we are dealing with smooth functions and kernels, in general the number of quadrature points required increases monotonically with $|x-y|$. For $m < M$ (D2) is smaller than (D1), which shows that Nyström's method is more efficient for small to moderate values of $|x-y|$ and moderate to large number of particles (or equivalently, at higher temperatures). When M is small and $|x-y|$ is large, the overlaps method is more efficient.

The middle column of Fig. 7 presents the evaluation time of $\rho^{(1)}(x, 2|2\Delta t)$ at different temperatures for a bosonic system of $N=10$ particles in the quantum Newton's cradle setup characterized by $l_{HO} = 0.56$, $\omega = 3$, $q = 4\pi$, $A = 1.5$, and $\Delta t = \pi/40\omega$. The evaluation times are obtained by increasing the number of quadrature points until the relative difference between two successive evaluations is smaller than 0.5×10^{-3} . At zero temperature ($M = N - 1$), from Fig. 7(b) we can see that for small to moderate values of the spatial separation Nyström's method is more efficient ($t_N < t_O$), but the situation is reversed for large values of $|x-2|$. The last column of Fig. 7 presents the results for t_O/t_N . If $t_O/t_N > 1$ then Nyström's method is more efficient, and when $t_O/t_N < 1$

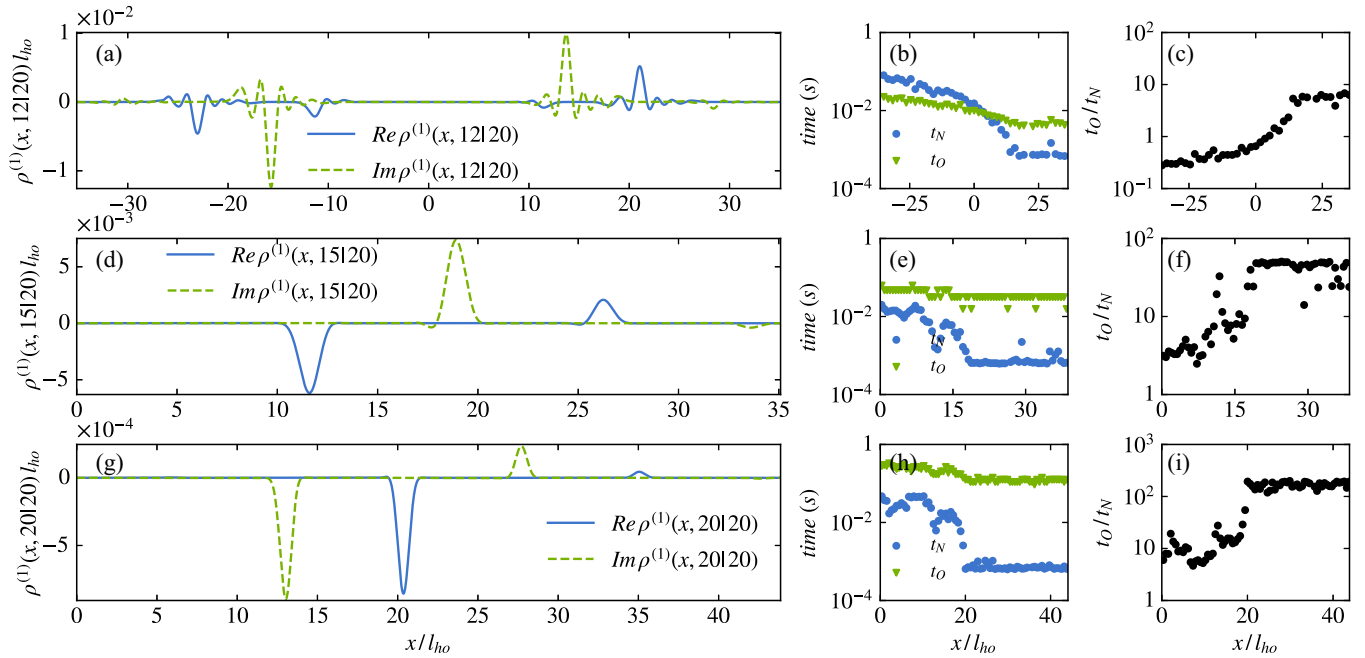


FIG. 8. The same quantities as in Fig. 7 for $t = 20\Delta t$ and $y = 12$ (a), $y = 15$ (d), and $y = 20$ (g).

the opposite is true. Already for $\theta_0 = 0.011$ when $M = 30$ we see from Fig. 7(e) that $t_O/t_N > 1$ for all values of x shown (outside of this interval the RDM is negligible), and for $\theta_0 = 0.0025$ [Fig. 7(h)] when $M = 60$ Nyström's method is almost everywhere more than ten times faster than the method based on the overlaps. Figure 8 presents similar re-

sults for the same setup at $t = 20\Delta t$ and $y = 12$ ($\theta_0 = 0$), $y = 15$ ($\theta_0 = 0.011$), and $y = 20$ ($\theta_0 = 0.025$). Even though the support of the RDM is now larger, the same conclusions can be drawn: with increasing M and temperature Nyström's method is far more efficient than the overlaps method.

- [1] J. M. Deutsch, Quantum statistical mechanics in a closed system, *Phys. Rev. A* **43**, 2046 (1991).
- [2] M. Srednicki, Chaos and quantum thermalization, *Phys. Rev. E* **50**, 888 (1994).
- [3] M. Rigol, V. Dunjko, and M. Olshanii, Thermalisation and its mechanism for generic isolated quantum systems, *Nature (London)* **452**, 854 (2008).
- [4] M. Rigol, V. Dunjko, V. Yurovsky, and M. Olshanii, Relaxation in a Completely Integrable Many-Body Quantum System: An Ab Initio Study of the Dynamics of the Highly Excited States of 1D Lattice Hard-Core Bosons, *Phys. Rev. Lett.* **98**, 050405 (2007).
- [5] L. Vidmar and M. Rigol, Generalized Gibbs ensemble in integrable lattice models, *J. Stat. Mech.* (2016) 064007.
- [6] E. Ilievski, J. De Nardis, B. Wouters, J.-S. Caux, F. H. L. Essler, and T. Prosen, Complete Generalized Gibbs Ensembles in an Interacting Theory, *Phys. Rev. Lett.* **115**, 157201 (2015).
- [7] E. Ilievski, E. Quinn, J. D. Nardis, and M. Brockmann, String-charge duality in integrable lattice models, *J. Stat. Mech.* (2016) 063101.
- [8] E. Ilievski, M. Medenjak, T. Prosen, and L. Zadnik, Quasilocal charges in integrable lattice systems, *J. Stat. Mech.* (2016) 064008.
- [9] M. Marcuzzi, J. Marino, A. Gambassi, and A. Silva, Prethermalization in a Nonintegrable Quantum Spin Chain after a Quench, *Phys. Rev. Lett.* **111**, 197203 (2013).
- [10] F. H. L. Essler, S. Kehrein, S. R. Manmana, and N. J. Robinson, Quench dynamics in a model with tuneable integrability breaking, *Phys. Rev. B* **89**, 165104 (2014).
- [11] G. P. Brandino, J.-S. Caux, and R. M. Konik, Glimmers of a Quantum KAM Theorem: Insights from Quantum Quenches in One-Dimensional Bose Gases, *Phys. Rev. X* **5**, 041043 (2015).
- [12] B. Bertini and M. Fagotti, Pre-relaxation in weakly interacting models, *J. Stat. Mech.* (2015) P07012.
- [13] B. Bertini, F. H. L. Essler, S. Groha, and N. J. Robinson, Prethermalization and Thermalization in Models with Weak Integrability Breaking, *Phys. Rev. Lett.* **115**, 180601 (2015).
- [14] M. Marcuzzi, J. Marino, A. Gambassi, and A. Silva, Prethermalization from a low-density Holstein-Primakov expansion, *Phys. Rev. B* **94**, 214304 (2016).
- [15] T. Langen, T. Gasenzer, and J. Schmiedmayer, Prethermalisation and universal dynamics in near-integrable quantum systems, *J. Stat. Mech.* (2016) 064009.
- [16] V. Alba and M. Fagotti, Prethermalization at Low Temperature: The Scent of a Spontaneously Broken Symmetry, *Phys. Rev. Lett.* **119**, 010601 (2017).
- [17] S. Hofferberth, I. Lesanovsky, B. Fischer, T. Schumm, and J. Schmiedmayer, Non-equilibrium coherence dynamics in one-dimensional Bose gases, *Nature (London)* **449**, 324 (2007).
- [18] S. Trotzky, Y.-A. Chen, A. Fleisch, I. P. McCulloch, U. Schollwöck, J. Eisert, and I. Bloch, Probing the relaxation

- towards equilibrium in an isolated strongly correlated 1D Bose gas, *Nat. Phys.* **8**, 325 (2012).
- [19] M. Gring, M. Kuhnert, T. Langen, T. Kitagawa, B. Rauer, M. Schreitl, I. Mazets, D. A. Smith, E. Demler, and J. Schmiedmayer, Relaxation and pre-thermalization in an isolated quantum system, *Science* **337**, 1318 (2012).
- [20] T. Langen, R. Geiger, M. Kuhnert, B. Rauer, and J. Schmiedmayer, Local emergence of thermal correlations in an isolated quantum many-body system, *Nat. Phys.* **9**, 640 (2013).
- [21] T. Langen, S. Erne, R. Geiger, B. Rauer, T. Schweigler, M. Kuhnert, W. Rohringer, I. E. Mazets, T. Gasenzer, and J. Schmiedmayer, Experimental observation of a generalized Gibbs ensemble, *Science* **348**, 207 (2015).
- [22] E. Nicklas, M. Karl, M. Höfer, A. Johnson, W. Muessel, H. Strobel, J. Tomkovič, T. Gasenzer, and M. K. Oberthaler, Observation of Scaling in the Dynamics of a Strongly Quenched Quantum Gas, *Phys. Rev. Lett.* **115**, 245301 (2015).
- [23] M. Cheneau, P. Barmettler, D. Poletti, M. Endres, P. Schauß, T. Fukuhara, C. Gross, I. Bloch, C. Kollath, and S. Kuhr, Light-cone-like spreading of correlations in a quantum many-body system, *Nature (London)* **481**, 484 (2012).
- [24] J. P. Ronzheimer, M. Schreiber, S. Braun, S. S. Hodgman, S. Langer, I. P. McCulloch, F. Heidrich-Meisner, I. Bloch, and U. Schneider, Expansion Dynamics of Interacting Bosons in Homogeneous Lattices in One and Two Dimensions, *Phys. Rev. Lett.* **110**, 205301 (2013).
- [25] B. Fang, G. Carleo, A. Johnson, and I. Bouchoule, Quench-Induced Breathing Mode of One-Dimensional Bose Gases, *Phys. Rev. Lett.* **113**, 035301 (2014); **116**, 169901(E) (2016).
- [26] T. Kinoshita, T. Wenger, and D. S. Weiss, A quantum Newton's cradle, *Nature (London)* **440**, 900 (2006).
- [27] E. H. Lieb and W. Liniger, Exact analysis of an interacting Bose gas, I. The general solution and the ground state, *Phys. Rev.* **130**, 1605 (1963).
- [28] E. H. Lieb, Exact analysis of an interacting Bose gas, II. The excitation spectrum, *Phys. Rev.* **130**, 1616 (1963).
- [29] V. E. Korepin, N. M. Bogoliubov, and A. G. Izergin, *Quantum Inverse Scattering Method and Correlation Functions* (Cambridge University Press, Cambridge, England, 1993).
- [30] M. Girardeau, Relationship between systems of impenetrable bosons and fermions in one dimension, *J. Math. Phys.* **1**, 516 (1960).
- [31] A. G. Rojo, J. L. Cohen, and P. R. Berman, Talbot oscillations and periodic focusing in a one-dimensional condensate, *Phys. Rev. A* **60**, 1482 (1999).
- [32] M. D. Girardeau, E. M. Wright, and J. M. Triscari, Ground-state properties of a one-dimensional system of hard-core bosons in a harmonic trap, *Phys. Rev. A* **63**, 033601 (2001).
- [33] M. D. Girardeau and E. M. Wright, Breakdown of Time-Dependent Mean-Field Theory for a One-Dimensional Condensate of Impenetrable Bosons, *Phys. Rev. Lett.* **84**, 5239 (2000).
- [34] M. D. Girardeau and E. M. Wright, Dark Solitons in a One-Dimensional Condensate of Hard Core Bosons, *Phys. Rev. Lett.* **84**, 5691 (2000).
- [35] K. K. Das, M. D. Girardeau, and E. M. Wright, Interference of a Thermal Tonks Gas on a Ring, *Phys. Rev. Lett.* **89**, 170404 (2002).
- [36] V. I. Yukalov and M. D. Girardeau, Fermi-Bose mapping for one-dimensional Bose gases, *Laser Phys. Lett.* **2**, 375 (2005).
- [37] A. Kundu, Exact Solution of Double δ Function Bose Gas through an Interacting Anyon Gas, *Phys. Rev. Lett.* **83**, 1275 (1999).
- [38] M. T. Batchelor, X.-W. Guan, and N. Oelkers, One-Dimensional Interacting Anyon Gas: Low-Energy Properties and Haldane Exclusion Statistics, *Phys. Rev. Lett.* **96**, 210402 (2006).
- [39] M. T. Batchelor, X.-W. Guan, and J.-S. He, The Bethe ansatz for 1D interacting anyons, *J. Stat. Mech.* (2007) P03007.
- [40] Y. Hao, Y. Zhang, and S. Chen, Ground-state properties of one-dimensional anyon gases, *Phys. Rev. A* **78**, 023631 (2008).
- [41] L. Piroli, S. Scopa, and P. Calabrese, Determinant formula for the field form factor in the anyonic Lieb-Liniger model, *J. Phys. A: Math. Theor.* **53**, 405001 (2020).
- [42] P. Calabrese and M. Mintchev, Correlation functions of one-dimensional anyonic fluids, *Phys. Rev. B* **75**, 233104 (2007).
- [43] O. I. Pătu, V. E. Korepin, and D. V. Averin, Correlation functions of one-dimensional Lieb-Liniger anyons, *J. Phys. A* **40**, 14963 (2007).
- [44] R. Santachiara and P. Calabrese, One-particle density matrix and momentum distribution function of one-dimensional anyon gases, *J. Stat. Mech.* (2008) P06005.
- [45] P. Calabrese and R. Santachiara, Off-diagonal correlations in one-dimensional anyonic models: A replica approach, *J. Stat. Mech.* (2009) P03002.
- [46] O. I. Pătu, V. E. Korepin, and D. V. Averin, One-dimensional impenetrable anyons in thermal equilibrium, III. Large distance asymptotics of the space correlations, *J. Phys. A* **42**, 275207 (2009).
- [47] O. I. Pătu, V. E. Korepin, and D. V. Averin, One-dimensional impenetrable anyons in thermal equilibrium, IV. Large time and distance asymptotic behavior of the correlation functions, *J. Phys. A* **43**, 115204 (2010).
- [48] G. Marmorini, M. Pepe, and P. Calabrese, One-body reduced density matrix of trapped impenetrable anyons in one dimension, *J. Stat. Mech.* (2016) 073106.
- [49] Y. Hao and Y. Song, One-dimensional hard-core anyon gas in a harmonic trap at finite temperature, *Eur. Phys. J. D* **71**, 135 (2017).
- [50] S. Scopa, L. Piroli, and P. Calabrese, One-particle density matrix of a trapped Lieb-Liniger anyonic gas, *J. Stat. Mech.* (2020) 093103.
- [51] R. Santachiara, F. Stauffer, and D. C. Cabra, Entanglement properties and momentum distributions of hard-core anyons on a ring, *J. Stat. Mech.* (2007) L05003.
- [52] H. Guo, Y. Hao, and S. Chen, Quantum entanglement of particles on a ring with fractional statistics, *Phys. Rev. A* **80**, 052332 (2009).
- [53] A. del Campo, Fermionization and bosonization of expanding one-dimensional anyonic fluids, *Phys. Rev. A* **78**, 045602 (2008).
- [54] T. M. Wright, M. Rigol, M. J. Davis, and K. V. Kheruntsyan, Nonequilibrium Dynamics of One-Dimensional Hard-Core Anyons Following a Quench: Complete Relaxation of One-Body Observables, *Phys. Rev. Lett.* **113**, 050601 (2014).
- [55] L. Piroli and P. Calabrese, Exact dynamics following an interaction quench in a one-dimensional anyonic gas, *Phys. Rev. A* **96**, 023611 (2017).

- [56] T. Keilmann, S. Lanzmich, I. McCulloch, and M. Roncaglia, Statistically induced phase transitions and anyons in 1D optical lattices, *Nat. Commun.* **2**, 361 (2011).
- [57] S. Greschner and L. Santos, Anyon Hubbard Model in One-Dimensional Optical Lattices, *Phys. Rev. Lett.* **115**, 053002 (2015).
- [58] C. Sträter, S. C. L. Srivastava, and A. Eckardt, Floquet Realization and Signatures of One-Dimensional Anyons in an Optical Lattice, *Phys. Rev. Lett.* **117**, 205303 (2016).
- [59] L. Cardarelli, S. Greschner, and L. Santos, Engineering interactions and anyon statistics by multicolor lattice depth modulations, *Phys. Rev. A* **94**, 023615 (2016).
- [60] S. Greschner, L. Cardarelli, and L. Santos, Probing the exchange statistics of one-dimensional anyon models, *Phys. Rev. A* **97**, 053605 (2018).
- [61] N. Ilieva and W. Thirring, Do anyons solve Heisenberg's Urgleichung in one dimension, *Eur. Phys. J. C* **6**, 705 (1999).
- [62] N. Ilieva and W. Thirring, Anyons and the Bose-Fermi duality in the finite-temperature Thirring model, *Theor. Math. Phys.* **121**, 1294 (1999).
- [63] D. V. Averin and J. A. Nesteroff, Coulomb Blockade of Anyons in Quantum Antidots, *Phys. Rev. Lett.* **99**, 096801 (2007).
- [64] M. D. Girardeau, Anyon-Fermion Mapping and Applications to Ultracold Gases in Tight Waveguides, *Phys. Rev. Lett.* **97**, 100402 (2006).
- [65] O. I. Pățu, V. E. Korepin, and D. V. Averin, One-dimensional impenetrable anyons in thermal equilibrium, I. Anyonic generalization of Lenard's formula, *J. Phys. A* **41**, 145006 (2008).
- [66] A. Liguori, M. Mintchev, and L. Pilo, Bosonization at finite temperature and anyon condensation, *Nucl. Phys. B* **569**, 577 (2000).
- [67] M. T. Batchelor, X.-W. Guan, and A. Kundu, One-dimensional anyons with competing δ -function and derivative δ -function potentials, *J. Phys. A* **41**, 352002 (2008).
- [68] M. T. Batchelor, A. Foerster, X.-W. Guan, J. Links, and H.-Q. Zhou, Quantum inverse scattering Method with anyonic grading, *J. Phys. A* **41**, 465201 (2008).
- [69] B. Bellazzini, P. Calabrese, and M. Mintchev, Junctions of anyonic Luttinger wires, *Phys. Rev. B* **79**, 085122 (2009).
- [70] M. Greiter, Statistical phases and momentum spacings for one-dimensional anyons, *Phys. Rev. B* **79**, 064409 (2009).
- [71] A. Kundu, Quantum integrable 1D anyonic models: Construction through braided Yang-Baxter equation, *SIGMA* **6**, 080 (2010).
- [72] A. Colcelli, G. Mussardo, and A. Trombettoni, Deviations from off-diagonal long-range order in one-dimensional quantum systems, *Europhys. Lett.* **122**, 50006 (2018).
- [73] B. Bellazzini, Dualities for anyons, *J. Phys. A* **44**, 035403 (2011).
- [74] C. D. Batista and R. D. Somma, Condensation of Anyons in Frustrated Quantum Magnets, *Phys. Rev. Lett.* **109**, 227203 (2012).
- [75] A. Rahmani, A. E. Feiguin, and C. D. Batista, Anyonic Liquids in Nearly Saturated Spin Chains, *Phys. Rev. Lett.* **113**, 267201 (2014).
- [76] L. Wang, L. Wang, and Y. Zhang, Quantum walks of two interacting anyons in one-dimensional optical lattices, *Phys. Rev. A* **90**, 063618 (2014).
- [77] M. Mintchev and P. Sorba, Luttinger liquid in non-equilibrium steady state, *J. Phys. A* **46**, 095006 (2013).
- [78] Y. Li and Z. He, Effect of inter-particle interactions on pair correlations of one-dimensional anyon gases, *J. Low Temp. Phys.* **181**, 49 (2015).
- [79] T. Dubček, B. Klajn, R. Pezer, H. Buljan, and D. Jukić, Quasimomentum distribution and expansion of an anyonic gas, *Phys. Rev. A* **97**, 011601(R) (2018).
- [80] D. Rossini, M. Carrega, M. C. Strinati, and L. Mazza, Anyonic tight-binding models of parafermions and of fractionalized fermions, *Phys. Rev. B* **99**, 085113 (2019).
- [81] N. L. Harshman and A. C. Knapp, Anyons from three-body hard-core interactions in one dimension, *Ann. Phys. (NY)* **412**, 168003 (2020).
- [82] L. Yang and H. Pu, One-body density matrix and momentum distribution of strongly interacting one-dimensional spinor quantum gases, *Phys. Rev. A* **95**, 051602(R) (2017).
- [83] Y.-L. Yao, J.-P. Cao, G.-L. Li, and H. Fan, Exact solutions of a multi-component anyon model with SU(N) invariance, *J. Phys. A* **45**, 045207 (2012).
- [84] R. A. Santos, F. N. C. Paraan, and V. E. Korepin, Quantum phase transition in a multicomponent anyonic Lieb-Liniger model, *Phys. Rev. B* **86**, 045123 (2012).
- [85] O. I. Pățu, Correlation functions and momentum distribution of one-dimensional hard-core anyons in optical lattices, *J. Stat. Mech.* (2015) P01004.
- [86] O. I. Pățu, Correlation functions of one-dimensional strongly interacting two-component gases, *Phys. Rev. A* **100**, 063635 (2019).
- [87] N. T. Zinner, Strongly interacting mesoscopic systems of anyons in one dimension, *Phys. Rev. A* **92**, 063634 (2015); **93**, 049901(E) (2016).
- [88] O. Gamayun, O. Lychkovskiy, and M. B. Zvonarev, Zero temperature momentum distribution of an impurity in a polaron state of one-dimensional Fermi and Tonks-Girardeau gases, *SciPost Phys.* **8**, 053 (2020).
- [89] M. Mintchev and P. Sorba, Anyon quantum transport and noise away from equilibrium, *Ann. Phys.* **20**, 2000276 (2020).
- [90] Y. Hao, Y. Zhang, and S. Chen, Ground-state properties of hard-core anyons in one-dimensional optical lattices, *Phys. Rev. A* **79**, 043633 (2009).
- [91] Y. Hao and S. Chen, Dynamical properties of hard-core anyons in one-dimensional optical lattices, *Phys. Rev. A* **86**, 043631 (2012).
- [92] Y. Hao, Ground-state properties of hard-core anyons in a harmonic potential, *Phys. Rev. A* **93**, 063627 (2016).
- [93] W. Zhang, S. Greschner, E. Fan, T. C. Scott, and Y. Zhang, Ground-state properties of the one-dimensional unconstrained pseudo-anyon Hubbard model, *Phys. Rev. A* **95**, 053614 (2017).
- [94] J. Arcila-Forero, R. Franco, and J. Silva-Valencia, Critical points of the anyon-Hubbard model, *Phys. Rev. A* **94**, 013611 (2016).
- [95] J. Arcila-Forero, R. Franco, and J. Silva-Valencia, Three-body-interaction effects on the ground state of one-dimensional anyons, *Phys. Rev. A* **97**, 023631 (2018).
- [96] R. Pezer and H. Buljan, Momentum Distribution Dynamics of a Tonks-Girardeau Gas: Bragg Reflections of a Quantum Many-Body Wave Packet, *Phys. Rev. Lett.* **98**, 240403 (2007).

- [97] Y. Y. Atas, D. M. Gangardt, I. Bouchoule, and K. V. Kheruntsyan, Exact nonequilibrium dynamics of finite-temperature Tonks-Girardeau gases, *Phys. Rev. A* **95**, 043622 (2017).
- [98] L. Vidmar, W. Xu, and M. Rigol, Emergent eigenstate solution and emergent Gibbs ensemble for expansion dynamics in optical lattices, *Phys. Rev. A* **96**, 013608 (2017).
- [99] A. Lenard, One-dimensional impenetrable bosons in thermal Equilibrium, *J. Math. Phys.* **7**, 1268 (1966).
- [100] W. H. Press, B. P. Flannery, S. A. Teukolsky, and W. T. Vetterling, *Numerical Recipes in C: The Art of Scientific Computing* (Cambridge University Press, Cambridge, England, 1992).
- [101] F. Bornemann, On the numerical evaluation of Fredholm determinants, *Math. Comput.* **79**, 871 (2010).
- [102] R. van den Berg, B. Wouters, S. Eliëns, J. De Nardis, R. M. Konik, and J.-S. Caux, Separation of Time Scales in a Quantum Newton's Cradle, *Phys. Rev. Lett.* **116**, 225302 (2016).
- [103] Y. Y. Atas, I. Bouchoule, D. M. Gangardt, and K. V. Kheruntsyan, Collective many-body bounce in the breathing-mode oscillations of a Tonks-Girardeau gas, *Phys. Rev. A* **96**, 041605(R) (2017).
- [104] W. Xu and M. Rigol, Expansion of one-dimensional lattice hard-core bosons at finite temperature, *Phys. Rev. A* **95**, 033617 (2017).
- [105] P. Vignolo and A. Minguzzi, Universal Contact for a Tonks-Girardeau Gas at Finite Temperature, *Phys. Rev. Lett.* **110**, 020403 (2013).
- [106] P. J. Forrester, N. E. Frankel, T. M. Garoni, and N. S. Witte, Finite one-dimensional impenetrable Bose systems: Occupation numbers, *Phys. Rev. A* **67**, 043607 (2003).
- [107] P. J. Forrester, N. E. Frankel, T. M. Garoni, and N. S. Witte, Painlevé transcendent evaluations of finite system density matrices for 1D impenetrable bosons, *Commun. Math. Phys.* **238**, 257 (2003).
- [108] P. Calabrese, M. Mintchev, and E. Vicari, The entanglement entropy of 1D systems in continuous and homogenous space, *J. Stat. Mech.* (2011) P09028.
- [109] C. Li, T. Zhou, I. Mazets, H.-P. Stimming, Z. Zhu, Y. Zhai, W. Xiong, X. Zhou, X. Chen, and J. Schmiedmayer, Dephasing and relaxation of bosons in 1D: Newton's cradle revisited, [arXiv:1804.01969](https://arxiv.org/abs/1804.01969).
- [110] Y. Tang, W. Kao, K.-Y. Li, S. Seo, K. Mallayya, M. Rigol, S. Gopalakrishnan, and B. L. Lev, Thermalization Near Integrability in a Dipolar Quantum Newton's Cradle, *Phys. Rev. X* **8**, 021030 (2018).
- [111] J.-S. Caux and F. H. L. Essler, Time Evolution of Local Observables After Quenching to an Integrable Model, *Phys. Rev. Lett.* **110**, 257203 (2013).
- [112] J.-S. Caux, The quench action, *J. Stat. Mech.* (2016) 064006.
- [113] O. A. Castro-Alvaredo, B. Doyon, and T. Yoshimura, Emergent Hydrodynamics in Integrable Quantum Systems Out of Equilibrium, *Phys. Rev. X* **6**, 041065 (2016).
- [114] B. Bertini, M. Collura, J. De Nardis, and M. Fagotti, Transport in Out-of-Equilibrium XXZ Chains: Exact Profiles of Charges and Currents, *Phys. Rev. Lett.* **117**, 207201 (2016).
- [115] J.-S. Caux, B. Doyon, J. Dubail, R. Konik, and T. Yoshimura, Hydrodynamics of the interacting Bose gas in the quantum Newton cradle setup, *SciPost Phys.* **6**, 070 (2019).
- [116] M. Schemmer, I. Bouchoule, B. Doyon, and J. Dubail, Generalized Hydrodynamics on an Atom Chip, *Phys. Rev. Lett.* **122**, 090601 (2019).
- [117] J. J. Sakurai, *Modern Quantum Mechanics* (Addison-Wesley Publishing Company, Boston, MA, 1995).
- [118] M. Abramowitz and I. A. Stegun, *Handbook of Mathematical Functions with Formulas, Graphs, and Mathematical Tables* (Dover Publications, Mineola, MN, 1964).
- [119] I. S. Gradshteyn and I. M. Ryzhik, *Table of Integrals, Series, and Products* (Elsevier/Academic Press, Amsterdam, Netherlands, 2007).
- [120] A. Minguzzi and D. M. Gangardt, Exact Coherent States of a Harmonically Confined Tonks-Girardeau Gas, *Phys. Rev. Lett.* **94**, 240404 (2005).
- [121] V. S. Popov and A. M. Perelomov, Parametric excitation of a quantum oscillator II, *Zh. Eksp. Teor. Fiz.* **57**, 1684 (1970) [*JETP* **30**, 910 (1970)].
- [122] A. M. Perelomov and Y. B. Zel'dovich, *Quantum Mechanics: Selected Topics* (World Scientific, Singapore, 1998).
- [123] M. Collura, S. Sotiriadis, and P. Calabrese, Quench dynamics of a Tonks-Girardeau gas released from a harmonic trap, *J. Stat. Mech.* (2013) P09025.
- [124] P. Ruggiero, Y. Brun, and J. Dubail, Conformal field theory on top of a breathing one-dimensional gas of hard core bosons, *SciPost Phys.* **6**, 051 (2019).
- [125] J. C. Piquette, A method for symbolic evaluation of indefinite integrals containing special functions or their products, *J. Symbol. Comput.* **11**, 231 (1991).
- [126] P. Calabrese, P. Le Doussal, and S. N. Majumdar, Random matrices and entanglement entropy of trapped Fermi gases, *Phys. Rev. A* **91**, 012303 (2015).
- [127] J. Settimo, N. Lo Gullo, F. Plastina, and A. Minguzzi, Exact spectral function of a Tonks-Girardeau gas in a lattice, [arXiv:2005.13646](https://arxiv.org/abs/2005.13646).
- [128] R. Modak, V. Alba, and P. Calabrese, Entanglement revivals as a probe of scrambling in finite quantum systems, *J. Stat. Mech.* (2020) 083110.
- [129] Y. Y. Atas, A. Safavi-Naini, and K. V. Kheruntsyan, Nonequilibrium quantum thermodynamics of the Tonks-Girardeau gas, [arXiv:2005.07313](https://arxiv.org/abs/2005.07313).
- [130] W. Pogorzelski, *Integral Equations and their Applications* (Pergamon Press, Oxford, England, 1966), Vol. I.
- [131] V. I. Smirnov, *A Course of Higher Mathematics* (Pergamon Press, Oxford, England, 1964), Vol. IV.
- [132] W. A. Hurwitz, Note on the Fredholm determinant, *Bull. Am. Math. Soc.* **20**, 406 (1914).
- [133] J. Feinberg, Fredholm's minors of arbitrary order: Their representations as a determinant of resolvents and in terms of free fermions and an explicit formula for their functional derivative, *J. Phys. A* **37**, 6299 (2004).
- [134] P. Devillard, D. Chevallier, P. Vignolo, and M. Albert, Full counting statistics of the momentum occupation numbers of the Tonks-Girardeau gas, *Phys. Rev. A* **101**, 063604 (2020).
- [135] P. J. Forrester, Meet Andréief, Bordeaux 1886, and Andreev, Kharkov 1882-1883, *Random Matric.: Theor. Applic.* **8**, 1930001 (2019).
- [136] J. Waldvogel, Fast construction of the Fejér and Clenshaw-Curtis quadrature rules, *BIT Numer. Math.* **46**, 195 (2006).
- [137] L. N. Trefethen, Is Gauss quadrature better than Clenshaw-Curtis? *SIAM Rev.* **50**, 67 (2008).